

Thematic review series: Lipid Posttranslational Modifications

Prelamin A, Zmpste24, misshapen cell nuclei, and progeria—new evidence suggesting that protein farnesylation could be important for disease pathogenesis

Stephen G. Young,^{1,*} Loren G. Fong,^{*} and Susan Michaelis^{1,†}

Division of Cardiology,^{*} Department of Internal Medicine, University of California, Los Angeles, CA 90095; and Department of Cell Biology,[†] Johns Hopkins University School of Medicine, Baltimore, MD 21205

Abstract Prelamin A undergoes multistep processing to yield lamin A, a structural protein of the nuclear lamina. Prelamin A terminates with a CAAX motif, which triggers farnesylation of a C-terminal cysteine (the C of the CAAX motif), endoproteolytic release of the last three amino acids (the AAX), and methylation of the newly exposed farnesylcysteine residue. In addition, prelamin A is cleaved a second time, releasing 15 more residues from the C terminus (including the farnesylcysteine methyl ester), generating mature lamin A. This second cleavage step is carried out by an endoplasmic reticulum membrane protease, ZMPSTE24. Interest in the posttranslational processing of prelamin A has increased with the recognition that certain progeroid syndromes can be caused by mutations that lead to an accumulation of farnesyl-prelamin A. Recently, we showed that a key cellular phenotype of these progeroid disorders, misshapen cell nuclei, can be ameliorated by inhibitors of protein farnesylation, suggesting a potential strategy for treating these diseases. In this article, we review the posttranslational processing of prelamin A, describe several mouse models for progeroid syndromes, explain the mutations underlying several human progeroid syndromes, and summarize recent data showing that misshapen nuclei can be ameliorated by treating cells with protein farnesyltransferase inhibitors.—Young, S. G., L. G. Fong, and S. Michaelis. Prelamin A, Zmpste24, misshapen cell nuclei, and progeria—new evidence suggesting that protein farnesylation could be important for disease pathogenesis. *J. Lipid Res.* 2005. 46: 2531–2558.

Supplementary key words protein prenylation • laminopathy • aging • Ste24 • a-factor • lamin A/C

Many cellular proteins are enzymatically modified by the addition of a cholesterol biosynthetic intermediate, either a 15 carbon farnesyl or a 20 carbon geranylgeranyl lipid (1–4). This lipid modification, generally called protein

prenylation, is important for facilitating the binding of proteins to membrane surfaces. Two broad classes of prenylated proteins exist. The Rab GTPases, important for trafficking of proteins to specific membrane compartments within cells, are geranylgeranylated at a pair of C-terminal cysteines (5–8). A more abundant group of proteins terminate with a C-terminal CAAX motif and are either farnesylated or geranylgeranylated at a C-terminal cysteine (the C of the CAAX motif), then further modified by endoproteolytic processing and methylation of the C-terminal prenylcysteine (1, 2, 9, 10). Examples of prenylated CAAX proteins include regulatory proteins such as the Ras and Rho proteins, several nuclear lamins (prelamin A, lamin B1, and lamin B2), and the yeast mating pheromone a-factor.

In this article, we focus largely on prelamin A, a farnesylated CAAX protein that undergoes multistep processing to yield mature lamin A, a structural protein of the nuclear lamina (11–14). In addition to the aforementioned CAAX motif modifications, prelamin A undergoes an additional endoproteolytic cleavage reaction that produces mature lamin A; this cleavage step releases 15 amino acids from the C terminus of prelamin A, including the farnesylcysteine methyl ester. Hence, mature lamin A is not farnesylated.

Interest in prelamin A and its posttranslational processing has recently increased with the recognition that certain progeroid syndromes can be caused by mutations that lead to an intracellular accumulation of farnesylated and carboxyl methylated prelamin A (15, 16). Remarkably, at least one of the cellular phenotypes associated with these progeroid disorders, misshapen cell nuclei, can be reversed or ameliorated by inhibitors of protein farnesylation, suggesting a possible strategy for treating these disorders.

Manuscript received 14 September 2005.

Published, JLR Papers in Press, October 5, 2005.
DOI 10.1194/jlr.R500011-JLR200

¹ To whom correspondence should be addressed.
e-mail: sgyoung@mednet.ucla.edu (S.G.Y.);
michaelis@jhmi.edu (S.M.)

In this article, we review the posttranslational processing of prelamin A, describe a mouse model for human progeroid syndromes, explain the mutations underlying several human progeroid syndromes, and summarize recent data indicating that the misshapen nuclei in certain progeroid syndromes can be ameliorated by treating cells with protein farnesyltransferase inhibitors (FTIs).

All of the enzymes responsible for the processing of mammalian prelamin A were initially identified in *Saccharomyces cerevisiae*, an organism that does not express prelamin A. In yeast, these processing enzymes are essential for the biogenesis of a farnesylated mating pheromone, **a**-factor, from its precursor protein (17–24). Parallels between the posttranslational processing of the **a**-factor in yeast and prelamin A in mammals are both informative and intriguing. Therefore, we will begin this review by “backing up” to yeast and reviewing the biogenesis of yeast **a**-factor.

POSTTRANSLATIONAL MODIFICATIONS OF CAAX PROTEINS

CAAX proteins terminate with the amino acids CAAX, in which the C is a cysteine, the A residues are usually aliphatic amino acids, and the X can be one of many different residues (25, 26). The CAAX sequence triggers three sequential enzymatic modifications (Fig. 1) (1, 26). First, a 15 carbon farnesyl or a 20 carbon geranylgeranyl lipid is added to the thiol group of the cysteine by cytosolic protein prenyltransferases, either protein farnesyltransferase (FTase) or protein geranylgeranyltransferase type I (1, 26). In general, the cysteine is geranylgeranylated if the X is a leucine or phenylalanine; otherwise, it is farnesylated (1, 27). Prelamin A terminates in CSIM and therefore is farnesyl-

lated; lamin B1 and lamin B2 are also farnesylated. Next, the last three amino acids (i.e., the AAX of the CAAX motif) are removed by a prenylprotein-specific endoprotease in the endoplasmic reticulum (ER) membrane (1). After endoproteolysis, the newly exposed isoprenylcysteine is methylated by an ER membrane prenylprotein-specific methyltransferase, isoprenylcysteine carboxyl methyltransferase (Icmt, designated Ste14p in yeast) (28, 29).

The CAAX motif modifications render the C terminus of the protein more hydrophobic, facilitating the binding of proteins to membrane surfaces (17, 30). In addition, CAAX modifications have been shown to facilitate protein-protein interactions (shown both for yeast Ras and its effector and for **a**-factor and its receptor and transporter) (9, 17, 31, 32), enhance the metabolic stability of proteins (**a**-factor intermediates in yeast lacking FTase or Ste14p are degraded rapidly) (17, 32), and facilitate the targeting of proteins to specific sites within the cell (20, 33–36). For example, in yeast, Ras proteins that do not undergo endoproteolysis or carboxyl methylation are not properly localized to the plasma membrane (Fig. 2).

PROCESSING OF MATING PHEROMONES IN *S. CEREVISIAE*

The discovery of protein prenylation and carboxyl methylation arose from the structural analysis of the mating pheromones secreted by several relatively obscure heterobasidiomycetous jelly fungi (*Tremella mesenterica*, *Tremella brasiliensis*, and *Rhodospiridium toruloides*) (31, 37–39). The A-10 mating factor of *T. mesenterica* was found to contain an α -carboxyl methyl ester of a C-terminal cysteine residue, which was also modified by an S-farnesyl group (37,

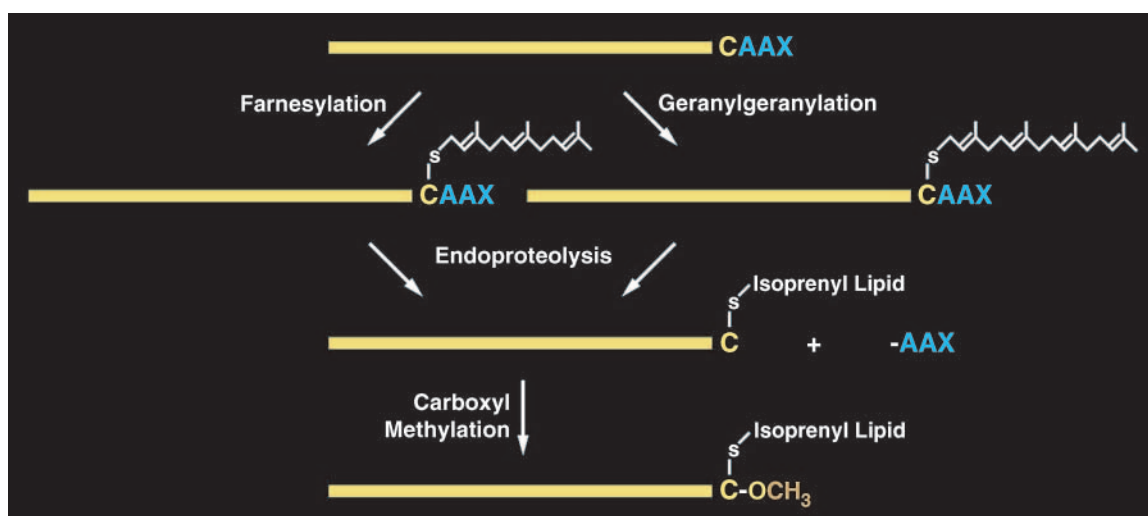


Fig. 1. Posttranslational processing of proteins that terminate with a C-terminal CAAX motif. CAAX proteins terminate with the amino acids CAAX, in which the C is a cysteine, the A residues are usually aliphatic amino acids, and the X can be one of many different residues. CAAX proteins undergo three sequential enzymatic modifications. First, a 15 carbon farnesyl or a 20 carbon geranylgeranyl lipid is added to the thiol group of the cysteine by protein prenyltransferases, either protein farnesyltransferase (FTase) or protein geranylgeranyltransferase type I. In general, the cysteine is geranylgeranylated if the X is a leucine or a phenylalanine; otherwise, it is farnesylated. Prelamin A terminates in CSIM; hence, it is farnesylated. Lamin B1, lamin B2, Ras proteins, and yeast **a**-factor are also farnesylated; the Rho and Rac proteins are geranylgeranylated.

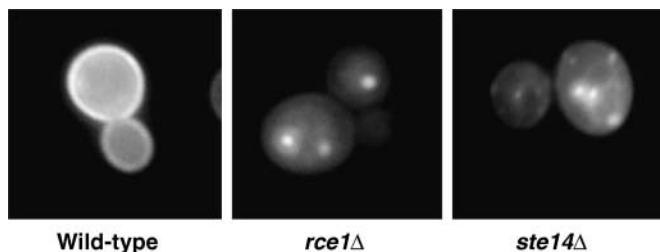


Fig. 2. Mislocalization of green fluorescent protein (GFP)-Ras2p in *rce1Δ* or *ste14Δ* yeast. The GFP-tagged Ras2p is at the plasma membrane in a wild-type strain but is mislocalized to internal membranes in the mutant *rce1Δ* and *ste14Δ* strains (20) (W. K. Schmidt and S. Michaelis, unpublished data).

38). Similar findings were made on the A(Ia) mating factor of *T. brasiliensis* (40, 41). All of the subsequent breakthroughs in understanding the CAAX processing machinery were made through the analysis of mating-defective mutants in *S. cerevisiae*. The mating process in *S. cerevisiae* (Fig. 3) involves two haploid cell types, *MATa* and *MATα*, which secrete the diffusible signaling molecules, **a**-factor and α -factor, respectively (42). The interaction of these mating pheromones with their cognate receptors leads to the formation of diploid yeast (Fig. 3). Despite the similarity in the function of **a**-factor and α -factor, the two pheromones are structurally and biochemically distinct. α -Factor is a nonlipidated peptide that is secreted by the classical secretory pathway, whereas **a**-factor is farnesylated and carboxyl methylated and is exported from yeast by a nonclassical secretion mechanism (18, 43–45).

Studies from our laboratory (17, 18, 21, 46–49) and others (19, 20) have provided a detailed view of the **a**-factor

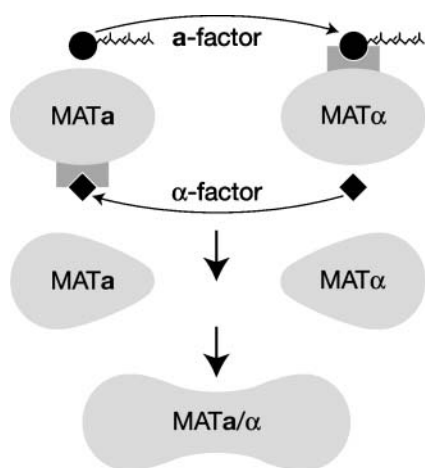


Fig. 3. Scheme of *S. cerevisiae* mating. The haploid yeast cell types (*MATa* and *MATα*) secrete the **a**-factor and α -factor pheromones, respectively, which initiate the mating process by interacting with receptors on the opposite cell type. The **a**-factor pheromone is a farnesylated and carboxyl methylated 12-mer, whereas α -factor is an unmodified 11-mer peptide (top) (42, 43). The pheromone-receptor interaction stimulates a signaling pathway that leads to G1 cell cycle arrest and morphological alteration called shmoo formation (middle). Ultimately, the haploid cells fuse at the shmoo tips to form the *MATa/α* diploid zygote (bottom), and the cell cycle resumes (42).

biogenesis pathway (Fig. 4). Despite the small size of **a**-factor (the precursor and mature forms are 36 and 12 amino acids, respectively), the **a**-factor biogenesis pathway is complex, comprising three major events: C-terminal processing of the CAAX motif of the **a**-factor precursor (Fig. 4, steps 1–3), proteolytic removal of the N-terminal extension (steps 4 and 5), and secretion of mature bioactive **a**-factor (step 6) via an ATP binding cassette transporter, Ste6p.

IDENTIFICATION OF ENZYMES RESPONSIBLE FOR THE C-TERMINAL PROCESSING OF A-FACTOR

A major breakthrough in the CAAX processing field was the discovery of the *RAM1* gene, which was identified in independent mutant screens as a suppressor of hyperactive Ras (*supH*) and as a mutant that was completely defective in mating and in the production of **a**-factor (*ste16*) (23, 44). The identification of *RAM1* (named for Ras and **a**-factor maturation) in entirely different genetic screens suggested a commonality between Ras and **a**-factor (23, 50). This commonality was underscored by the presence of a CAAX motif in both proteins. Ultimately, both Ras and **a**-factor were shown to be prenylated and methylated, and *RAM1*, along with a second gene, *RAM2*, was shown to encode different subunits of a heterodimeric enzyme, protein farnesyltransferase (24).

Ras and **a**-factor also require the same gene, *STE14*, for carboxyl methylation (Fig. 4, step 3). *STE14* encodes an ICMT. This gene was initially identified by characterizing a sterile strain of yeast, *ste14Δ*, that lacked the capacity to produce a functional **a**-factor (21, 22, 32). Because Ste14p is an integral membrane protein of the ER membrane, the purification of the enzyme presented major challenges. However, heterologous expression studies (21, 51), and ultimately biochemical experiments with a purified Ste14p enzyme (52), demonstrated that Ste14p is indeed an ICMT and that it is the sole enzyme for methylating CAAX proteins in yeast.

Interestingly, the genes encoding CAAX endoprotease enzymes (Fig. 4, step 2) were never identified in standard genetic screens for sterile yeast defective in **a**-factor production. In hindsight, the failure to identify the endoproteases by simple genetic screens was entirely predictable, as we now know that two functionally redundant CAAX endoproteases exist in yeast, Ste24p and Rce1p, and both are capable of participating in the cleavage of the AAX from **a**-factor (20). Thus, a mutation in a single gene could not be expected to yield a sterile phenotype. The key to discovering *RCE1* and *AFC1* (another name for *STE24*) rested on experiments performed by Boyartchuk, Ashby, and Rine (20) with an **a**-factor substrate that could be cleaved by Ste24p but not by Rce1p. They produced yeast expressing a mutant form of **a**-factor terminating in CAMQ rather than with the wild-type CVIA motif and demonstrated that the yeast remained capable of producing mature **a**-factor. The mutant yeast expressing the CAMQ version of **a**-factor were then mutagenized, and an autocrine arrest selection

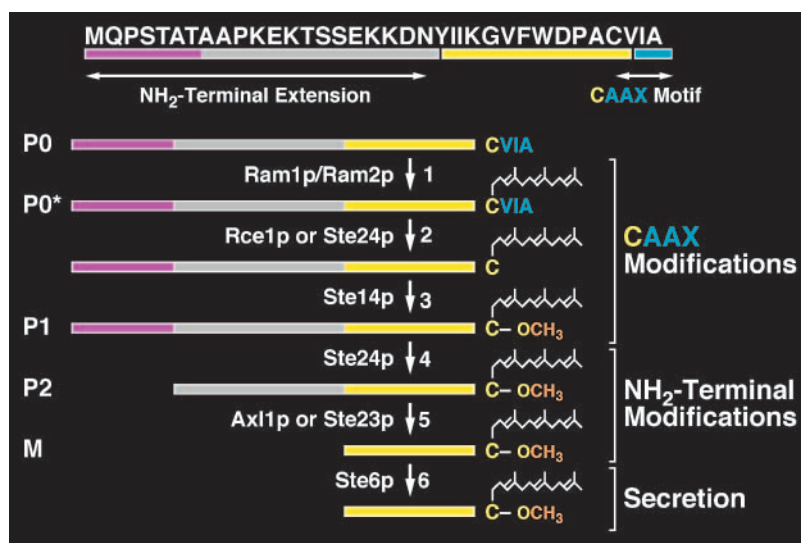


Fig. 4. Scheme of **a**-factor biogenesis. The **a**-factor precursor (P0) contains a C-terminal CAAX motif and an N-terminal extension and is encoded by the functionally redundant genes *MFA1* (whose product is shown here) and *MFA2*. The CAAX motif directs an ordered series of C-terminal modifications (farnesylation, endoproteolytic cleavage, and carboxyl methylation; steps 1–3). The N-terminal extension undergoes two sequential proteolytic cleavages (steps 4 and 5). These modifications yield mature **a**-factor, a farnesylated and carboxyl methylated dodecapeptide (M), which is exported from the cell (step 6) by an ATP binding cassette transporter, Ste6p. The precursor (P0), the biosynthetic intermediates (P0*, P1, P2), and mature **a**-factor (M) can be distinguished by SDS-PAGE (17, 18, 47, 48, 57). The gene products and corresponding enzymatic activities that mediate steps 1–6 of the **a**-factor biogenesis pathway are indicated. As described in the text, Ste24p has a role in two cleavage events associated with this pathway (steps 2 and 4). In its role as a CAAX protease, Ste24p performs a redundant function with Rce1p (step 2) to yield the P0* **a**-factor intermediate. As an N-terminal protease (step 4), Ste24p mediates the P1→P2 proteolytic cleavage. Both reactions can be carried out by purified Ste24p (49).

strategy was used to isolate sterile mutants (20). This approach resulted in the identification of a sterile yeast mutant, and the responsible gene, *STE24*, was cloned by complementation. *STE24* encodes a 453 amino acid protein, Ste24p, with multiple predicted transmembrane helices as well as an HEXXH (H, His; E, Glu) motif characteristic of a group of zinc-dependent metalloproteases (53). Mutating either of the conserved histidines in the HEXXH domain blocked the ability of Ste24p to complement the mating defect of *STE24*-deficient yeast (*ste24Δ*) expressing the CAMQ form of **a**-factor (20).

STE24-deficient yeast expressing wild-type **a**-factor secreted reduced amounts of **a**-factor but were not sterile, suggesting the existence of another gene capable of processing **a**-factor. The residual CAAX endoprotease activity in *ste24Δ* yeast membranes was insensitive to the zinc chelator 1,10-*o*-phenanthroline, suggesting that the remaining endoprotease was not a zinc metalloprotease (20). To isolate the remaining endoprotease, *ste24Δ* yeast were mutagenized and screened for a mutation that blocked residual **a**-factor production. This approach led to the identification of *RCE1*, which encodes a 329 amino acid protein that is also predicted to have multiple transmembrane helices (20). Unlike Ste24p, Rce1p does not contain sequences characteristic of any of the defined classes of proteases, but there were remote similarities with the type IIb signal peptidase (20). Yeast lacking *RCE1* (*rce1Δ*) manifest a modest decrease in **a**-factor production, and membranes from

rce1Δ yeast had moderately decreased CAAX endoprotease activity in *in vitro* assays with farnesylated **a**-factor peptide substrates. The residual CAAX endoprotease activity in *rce1Δ* yeast was sensitive to *o*-phenanthroline, consistent with Ste24p being a zinc metalloprotease (20).

The functional redundancy of Ste24p and Rce1p for processing **a**-factor with a wild-type CAAX motif can be readily demonstrated with a yeast halo assay (Fig. 5) (20, 54–56). In this assay, the production of mature **a**-factor can be visualized by a zone of growth inhibition (halo) in a lawn of yeast with an α -mating type. The single mutants (*ste24Δ* and *rce1Δ*) have modestly reduced **a**-factor production and therefore yield slightly smaller halos, whereas the double mutant (*ste24Δrce1Δ*) fails to carry out CAAX endoproteolysis, resulting in the complete inability to produce mature **a**-factor and the complete absence of a halo (Fig. 5).

Ste24p and Rce1p have different abilities to cleave **a**-factor mutants with different CAAX motifs. An **a**-factor mutant with the CAMQ sequence motif can only be cleaved by Ste24p, whereas other **a**-factor mutants, such as one terminating in CTLM, are cleaved solely by Rce1p (Fig. 5) (19). Notably, when the CAAX motif for mammalian prelamin A, CSIM, is tested in the **a**-factor assay, it is cleaved mainly by Rce1p (Fig. 5). The sequence specificities of Ste24p and Rce1p in the context of **a**-factor have been examined by Rine and colleagues (55). However, a complete picture of the specificities of these two enzymes has not yet emerged,

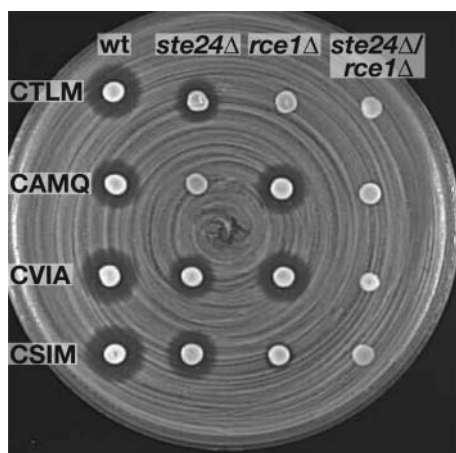


Fig. 5. The CAAX endoproteases Ste24p and Rce1p exhibit distinct, but overlapping, substrate specificities. Plasmids encoding the yeast **a**-factor gene (*MFAT*) with its normal CAAX motif (CVIA; row 3) or CAAX variants (rows 1, 2, and 4) were transformed into the indicated yeast strains that lack none [wild type (wt)], one (*ste24Δ* or *rce1Δ*), or both (*ste24Δrce1Δ*) of the CAAX endoprotease genes. The relative levels of **a**-factor produced by these strains were evaluated by the **a**-factor “halo assay.” In this assay, *MATα* cells are spotted onto a lawn of *MATα sst2* cells that are hypersensitive to **a**-factor. The zone of growth inhibition (halo) reflects the amount of **a**-factor produced by the cells that are spotted. Only properly processed **a**-factor results in a halo. The variants tested here, from top to bottom, are CTLM from Ste18p, which like the Ras2p CAAX motif (CIIS) is Rce1p-specific (20, 55); CAMQ from the mammalian phosphorylase kinase α subunit, which is Ste24p-specific (20); CVIA, the **a**-factor CAAX motif, which can be cleaved by either Rce1p or Ste24p (19, 20, 47); and CSIM, the prelamina CAAX motif, which appears to be Rce1p-specific (M. Boyle and S. Michaelis, unpublished data).

either for **a**-factor or for any other CAAX protein, and it is not clear whether any additional structural features, aside from the sequence of the CAAX motif, influence enzyme specificity.

A SECOND ROLE FOR *STE24* IN THE BIOGENESIS OF **A**-FACTOR

A surprising discovery, and one quite relevant to this review, was our finding that one of the **a**-factor-processing enzymes, Ste24p, actually plays dual roles in **a**-factor maturation. As shown in Fig. 4, Ste24p mediates both the C-terminal CAAX endoproteolysis (step 2) and the first N-terminal cleavage (step 4) (18–20, 47). In addition to the CAAX motif modifications on the C terminus of **a**-factor (farnesylation, endoproteolytic release of the AAX, and methylation), two additional endoprotease steps within the N-terminal portion of the molecule are required to generate mature **a**-factor. The first of these processing steps, which converts the P1 intermediate to P2, involves the endoproteolytic release of the first seven amino acids of the protein (17). This cleavage reaction was shown by Edman sequencing to occur between threonine-7 and alanine-8 and is blocked in an Ala8Gly **a**-factor mutant (18). The second cleavage reaction, which converts the P2 intermediate to

mature **a**-factor, involves the release of an additional 14 amino acids (17, 43).

Metabolic labeling experiments of wild-type yeast have shown that P1 is initially converted to P2, after which the P2 intermediate is further processed to mature **a**-factor (Fig. 4, steps 4 and 5) (17). Genetic experiments have shown that Axl1p plays a key role in the second of the two N-terminal processing steps, converting P2 to mature **a**-factor (57). In *axl1Δ* yeast, the P2 intermediate of **a**-factor accumulates. A search of the *S. cerevisiae* sequence database revealed a gene similar to *AXL1*, designated *STE23*, and this gene product can also participate in the second N-terminal proteolysis step. Yeast lacking *AXL1* have a reduced capacity to produce **a**-factor, whereas mutants lacking both *AXL1* and *STE23* (*axl1Δste23Δ*) are completely sterile (57).

Our studies revealed that the first of the two N-terminal cleavage reactions, the one that converts P1 to P2, is dependent on *STE24* and can be blocked by mutating the HEXXH motif in Ste24p (18). In the absence of *STE24*, the P1 intermediate accumulates (Fig. 6). Interestingly, this N-terminal cleavage reaction was the first role to be ascribed to Ste24p (18), followed soon thereafter by the report demonstrating the role of Ste24p in the release of the AAX (20). The apparent conflict posed by reports indicating different roles in **a**-factor biogenesis was quickly resolved by additional genetic and biochemical studies, which showed that Ste24p actually has dual roles in **a**-factor processing. Along with Rce1p, Ste24p is capable of releasing the AAX from **a**-factor; Ste24p also clearly cleaves the first seven amino acids from the protein (19, 47). Yeast lacking *STE24* exhibit a strikingly reduced capacity to produce mature **a**-factor; only a small amount of mature **a**-factor, perhaps 5% of the normal amount, is still made (18, 19). The most likely explanation for the residual **a**-factor production is that some Axl1p/Ste23p-mediated cleavage of **a**-factor occurs in the absence of Ste24p, albeit at reduced efficiency.

Neither the C- nor the N-terminal cleavage of **a**-factor occurs in the absence of farnesylation, as shown by the complete lack of proteolytic intermediates in *ram1Δ* or *ram2Δ* mutants (17, 24). Whether farnesylation is required for substrate recognition and specificity, or simply facilitates the recruitment of the **a**-factor intermediate to membranes containing Ste24p, has not yet been determined. However, the N-terminal cleavage reaction mediated by Ste24p does not require prior carboxyl methylation, because N-terminal cleavage occurs normally in yeast lacking *STE14* (32). The precise sequences and structures within the **a**-factor required for the two N-terminal cleavage reactions have not yet been determined, but with the experimental systems that have been developed, it should be possible to obtain that type of information.

Recently, a histidine-tagged version of Ste24p was detergent-solubilized and purified to homogeneity from yeast and shown to be the sole protein needed to mediate both the C- and N-terminal **a**-factor cleavage reactions (49). Given that fact that Ste24p is a membrane protein, the retention of enzymatic activities after purification was remarkable. Both of the activities were blocked by *o*-phenanthroline and reactivated by zinc (49).

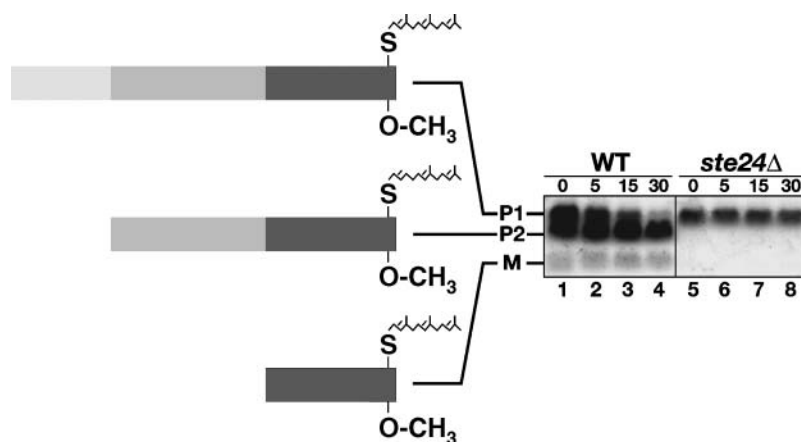


Fig. 6. The P1 intermediate of **a**-factor accumulates in *ste24Δ* yeast. The N-terminal (P1→P2) processing of **a**-factor is defective in a *ste24Δ* mutant. Processing of the **a**-factor precursor in wild-type (WT) and *ste24Δ* mutant cells is shown. Cells were pulse-labeled with [³⁵S]cysteine for 5 min and chased for 30 min. The intracellular fraction was subjected to immunoprecipitation with **a**-factor antibodies, electrophoresis, and autoradiography. The P1, P2, and M forms of **a**-factor are indicated. P1 accumulates in the *ste24Δ* mutant. This figure is adopted from *The Journal of Cell Biology* (18), and reproduced by copyright permission of Rockefeller University Press.

THE *STE24* ORTHOLOG IN MAMMALS, *ZMPSTE24*, COMPLEMENTS *STE24* DEFICIENCY IN YEAST

The genes encoding the mammalian postisoprenylation enzymes (*ZMPSTE24*, *RCE1*, and *ICMT*) were identified by homology with their yeast counterparts (*STE24*, *RCE1*, and *STE14*, respectively) (29, 47, 58). In each case, the mammalian gene complements the yeast mutant, as judged by a conventional **a**-factor halo assay and yeast mating tests. In this regard, our studies of human *ZMPSTE24* deserve special mention because we were able to demonstrate its ability to complement both the C- and N-terminal endoproteolytic processing reactions of **a**-factor (47). This point is illustrated in **Fig. 7**, in which complementation of *ste24Δrce1Δ* yeast with human *ZMPSTE24* is shown by three separate assays (metabolic labeling, halo, and mating). Mouse *Zmpste24* also fully complements the **a**-factor production defect in *ste24Δrce1Δ* yeast (see **Fig. 13A** below) (54). The complementation of the mutant yeast was fascinating, particularly because signaling molecules resembling **a**-factor have never been identified in mammals. Thus, mammalian *Zmpste24* retains the capacity to process a yeast substrate after nearly 800 million years of evolution. The ability of the mammalian enzyme to process yeast **a**-factor has facilitated the functional analysis of mutant forms of *ZMPSTE24* in humans (59).

It is worth pointing out that multiple names have been used in the literature for yeast *STE24* and mammalian *Zmpste24*. First cloned and named *STE24* in yeast (18), the gene was later called *AFC1* (for **a**-factor-converting enzyme) (20). Currently, the *STE24* designation is used exclusively by bioinformatics databases and the scientific community. Different names have also been applied to the mammalian gene *Zmpste24*. We cloned the first full-length mammalian version of *Zmpste24* and initially designated it *HsSTE24* (for *Homo sapiens STE24*) (47). Another group called it *HsSte24* (60). The official name for the human and mouse genes has since been changed to *Zmpste24*

(to reflect the fact that this enzyme is an ortholog of *Ste24p* and is a zinc metalloprotease). One group came up with entirely new names for *Ste24p/Zmpste24* and *Rce1*, calling them *FACE-1* and *FACE-2*, for farnesylated protein-converting enzymes 1 and 2, respectively (61). Those names were less than ideal choices, in our opinion, because it was well established at the time that at least one of the endoprotease activities, now recognized to be *Rce1*, processes both farnesylated and geranylgeranylated proteins, not just farnesylated proteins.

PHYSIOLOGIC IMPORTANCE OF *RCE1* AND *ICMT* IN MAMMALS AND MICE

Deciphering the physiologic importance of CAAX processing in mammals has been greatly aided by the development of *Rce1* and *Icmt* knockout mice (35, 62). Nearly all homozygous knockout mice (*Rce1*^{−/−}) died fairly late in gestation, beginning at embryonic day 14.5–15.5 (35). Very rarely, *Rce1*^{−/−} mice were born alive, but they were runted and lived for only a few weeks. *Rce1* deficiency had no significant effect on hematopoiesis, and the major organ systems of *Rce1*^{−/−} embryos were histologically normal late in gestation (35).

Rce1 is absolutely essential for the endoproteolytic processing of the Ras proteins in mice. The electrophoretic mobility of Ras proteins is distinctly abnormal in *Rce1*^{−/−} embryo lysates (35). Because endoproteolysis is a prerequisite for carboxyl methylation, we predicted that Ras proteins from *Rce1*^{−/−} fibroblasts would not be methylated. Indeed, this was the case. When we labeled *Rce1*^{+/+} and *Rce1*^{−/−} fibroblasts with L-[methyl-³H]methionine, the Ras proteins from *Rce1*^{+/+} fibroblasts contained a ³H-labeled farnesylcysteine methyl ester, whereas the Ras proteins from *Rce1*^{−/−} fibroblasts did not (35).

Crude membrane fractions from *Rce1*^{+/+} fibroblasts were capable of cleaving the AAX from recombinant H-Ras,

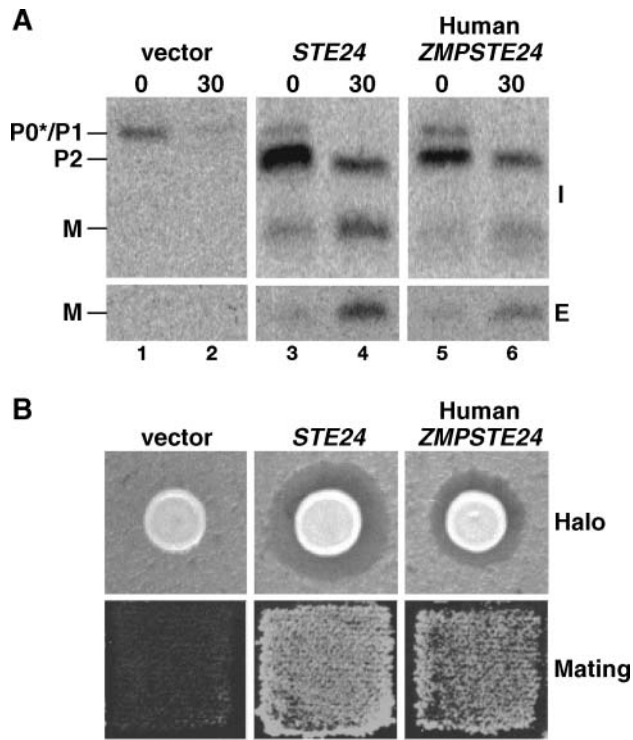


Fig. 7. The human *STE24* homolog, *ZMPSTE24*, complements the **a**-factor biosynthesis, halo, and mating defects when expressed in *ste24Δrce1Δ* mutant yeast. The human *ZMPSTE24* gene was tested in parallel with yeast *STE24* for its ability to complement the **a**-factor defect of a double (*ste24Δrce1Δ*) mutant strain. Using this mutant, the yeast or human protein must carry out both the C-terminal CAAX processing and N-terminal processing of **a**-factor to generate mature bioactive **a**-factor. Cells transformed with empty vector, yeast *STE24*, or human *ZMPSTE24* were tested for their ability to produce the P1, P2, and M (mature) **a**-factor in a metabolic labeling experiment (A) and in **a**-factor halo and mating assays (B) (47, 49). In the mating test, patches of auxotrophic *MATa* cells are replica-plated to a lawn of *MATα* cells with complementary auxotrophy. Where mating occurs, prototrophic diploids are formed that can grow in medium with no supplements. I, intracellular; E, extracellular. This figure is adapted from figures published in *The Journal of Cell Biology* (47) and *The Journal of Biological Chemistry* (48) and is reproduced with permission.

N-Ras, and K-Ras, regardless of whether they were farnesylated or geranylgeranylated (35, 58). In contrast, membranes from *Rce1*^{−/−} fibroblasts did not process any of the Ras proteins. Thus, as in yeast (20), the endoproteolytic processing of the Ras proteins requires Rce1. The endoproteolytic processing of other CAAX proteins was also blocked (35, 58). Interestingly, Rce1 is required for the endoproteolytic processing of lamin B1. Maske et al. (63) generated a monoclonal antibody specific for the C terminus of lamin B1, but the antibody did not bind unless the protein had undergone both farnesylation and endoproteolytic processing. Of note, the monoclonal antibody did not detect lamin B1 in *Rce1*^{−/−} fibroblasts, indicating that Rce1 is solely responsible for the processing of that protein. Because Rce1 has so many protein substrates, it was not surprising that biochemical studies revealed a substantial accumulation of uncleaved and unmethylated CAAX protein substrates in *Rce1*^{−/−} fibroblasts (54).

In *Rce1*^{+/+} fibroblasts, the Ras proteins are located along the inner surface of the plasma membrane, as judged by cell transfection experiments with green fluorescent protein (GFP)-Ras fusion constructs (35, 36). In contrast, the Ras proteins in *Rce1*^{−/−} fibroblasts were strikingly mislocalized to the cytosol and internal membrane compartments (35, 36), similar to what is seen in the yeast mutant (Fig. 2), underscoring the importance of endoproteolysis (and subsequent methylation) for proper membrane targeting.

The *Rce1* knockout had functionally important consequences. *Rce1*^{−/−} fibroblasts grew slightly more slowly than *Rce1*^{+/+} fibroblasts and were less susceptible to oncogenic transformation by activated forms of Ras (64). Also, we generated mice homozygous for a conditional *Rce1* allele and then showed that Cre-mediated inactivation of *Rce1* in fibroblasts reduces transformation by mutationally activated forms of Ras (64).

We also created mice lacking *Icmt* (33) and to our surprise found that this gene defect caused a more severe phenotype than *Rce1* deficiency. *Icmt*^{−/−} embryos were viable until E10.5, but they all died by E12.5. One study contended that *Icmt* might be particularly important for the development of the liver (65). *Icmt* also might be important for the development of the brain; *Icmt*^{−/−} embryonic stem (ES) cells completely lacked the ability to contribute to the formation of the brain (62).

We were successful in culturing *Icmt*^{−/−} fibroblasts from E11.5 mouse embryos (62). *Icmt*^{−/−} fibroblasts lacked methyltransferase activity against both small-molecule *Icmt* substrates (e.g., N-acetyl-farnesylcysteine) and farnesylated proteins such as K-Ras (33). *Icmt* deficiency led to a substantial accumulation of unmethylated *Icmt* protein substrates within cells (i.e., proteins susceptible to methylation in the presence of recombinant *Icmt* and the methyl donor S-adenosylmethionine) (33). *Icmt* is the only enzyme for methylating prenylcysteines in mammalian cells, methylating both CAAX proteins and the CXC subset (62, 66) of geranylgeranylated Rab proteins. Primary *Icmt*^{−/−} fibroblasts clearly grow more slowly than wild-type fibroblasts.

The Ras proteins in *Icmt*^{−/−} fibroblasts were not methylated, resulting in a very subtle retardation in electrophoretic mobility on SDS-polyacrylamide gels. Also, the Ras proteins were mislocalized in *Icmt*^{−/−} fibroblasts, as judged by transfection experiments with GFP-Ras fusion constructs (Fig. 8) (36, 62). Recent studies have shown that methylation is important for CAAX protein targeting within cells when the protein is farnesylated (36). When the CAAX protein is geranylgeranylated, the contribution of methylation to intracellular targeting appears to be negligible or nonexistent (36, 67).

We produced mice that are homozygous for a conditional *Icmt* allele (*Icmt*^{fl/fl}). Cre-mediated inactivation of *Icmt* mislocalized Ras proteins within cells, changed the steady-state concentration of both Rho and Ras proteins, and reduced the ability of mutationally activated Ras proteins to transform cultured fibroblasts (34). The latter finding has prompted interest in *Icmt* inhibitors as possible anticancer agents (68–70).

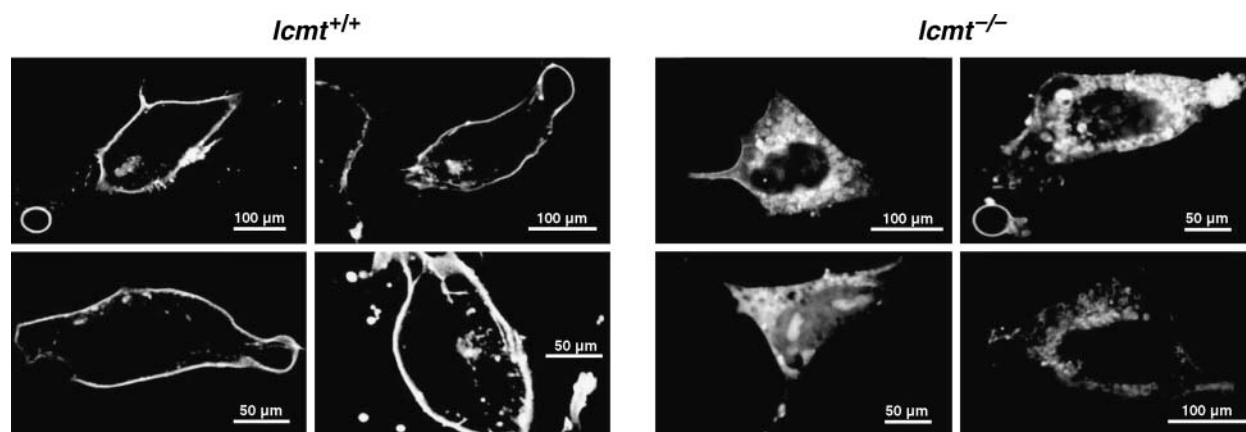


Fig. 8. Mislocalization of K-Ras in spontaneously immortalized *Icm1*^{-/-} fibroblasts that had been transfected with a GFP-K-Ras fusion construct (33, 34). The Ras proteins are similarly mislocalized in *Rce1*^{-/-} fibroblasts (35, 36). Several of these images have been published previously in *The Journal of Clinical Investigation* (34) and *The Enzymes* (115) and are reproduced with permission.

Previous pharmacologic studies with inhibitors of protein farnesyltransferase had shown that farnesylation is critical for the proper intracellular targeting of CAAX proteins (71–74). Studies with *Rce1*- and *Icm1*-deficient fibroblasts (9, 33–36, 62) have shown that the endoprotease and methyltransferase steps are also important for the proper targeting of some CAAX proteins in cells. We believe that these findings suggest a valuable lesson: whenever CAAX proteins are implicated in human disease, it is important to consider whether the disease might conceivably be treated by “attacking” the posttranslational modifications, thereby interfering with the localization and function of these proteins within cells.

NUCLEAR LAMINS: ABUNDANT MAMMALIAN CAAX PROTEINS

Lamin A, lamin C, lamin B1, and lamin B2 are intermediate filament proteins and are among the most abundant CAAX proteins in mammalian cells (1, 75–77). These proteins are key structural components of the nuclear lamina, a filamentous meshwork that lies beneath the inner nuclear membrane. Each of the lamin proteins contains an N-terminal globular domain, a central helical rod domain, and a C-terminal globular domain (12, 14). The lamin monomers dimerize to form parallel coiled-coil homodimers, which then associate head-to-tail to form strings and ultimately higher order 10 nm thick filaments that form the meshwork. It is unclear whether the different lamins form heterodimers. The nuclear lamins interact with a variety of integral membrane proteins of the inner nuclear membrane and also with transcription factors, as well as with heterochromatin itself (12, 78). Thus, these proteins have many roles besides simply forming a passive scaffold for the nuclear envelope.

Prelamin A, lamin B1, and lamin B2, but not lamin C, contain CAAX motifs and undergo the usual CAAX motif modifications (isoprenylation, endoproteolysis, and methylation) (Fig. 9). In the case of prelamin A, the release of

the AAX is likely a redundant function of Zmpste24 and Rce1 (79–81). As noted previously, however, prelamin A undergoes a second endoproteolytic processing step (82). The last 15 amino acids of the protein (including the farnesylcysteine methyl ester) are clipped off and degraded, leaving behind mature lamin A (Fig. 9). This second proteolytic processing step is carried out by Zmpste24 (81). In the absence of that enzyme, farnesyl-prelamin A accumulates within cells (Fig. 10), specifically at the nuclear envelope (Fig. 11) (16, 83).

Prelamin A and lamin C are products of the same gene (*Lmna*) and result from alternative splicing. The lamin C transcript terminates at the end of exon 10; the prelamin A transcript requires splicing from mid-exon 10 to exon 11, and then to exon 12 (11). Lamins A and C are identical for 566 amino acids but then diverge at the C-terminal domains (12, 13, 84). Lamin A contains 98 lamin A-specific amino acids at its C terminus, including the CAAX motif; lamin C, which lacks a CAAX motif, contains 6 unique amino acids at its C terminus.

Lamin B1 and lamin B2 contain nuclear localization motifs and are further targeted to the inner nuclear membrane by their C-terminal farnesylcysteine methyl ester (85, 86). Prelamin A is also targeted to the nucleus by a nuclear localization sequence; its farnesylcysteine methyl ester is important for targeting prelamin A to the inner nuclear membrane (87), where it almost certainly undergoes the second endoproteolytic processing step that releases mature lamin A (88). [Zmpste24 is an ER protein (46, 60), but we presume that continuities between the ER and the nuclear envelope mean that Zmpste24 may also be located along the inner nuclear membrane.] Noncleavable prelamin A mutants, which cannot undergo the second processing step, localize to the nuclear envelope (88). Prelamin A mutations that abrogate farnesylation (i.e., mutants in which the C of the CAAX motif is changed to another amino acid such as serine) do not prevent targeting to the nucleus, but the mutant protein remains largely in the nucleoplasm and fails to reach the nuclear envelope (88). Interestingly, one report has suggested that the

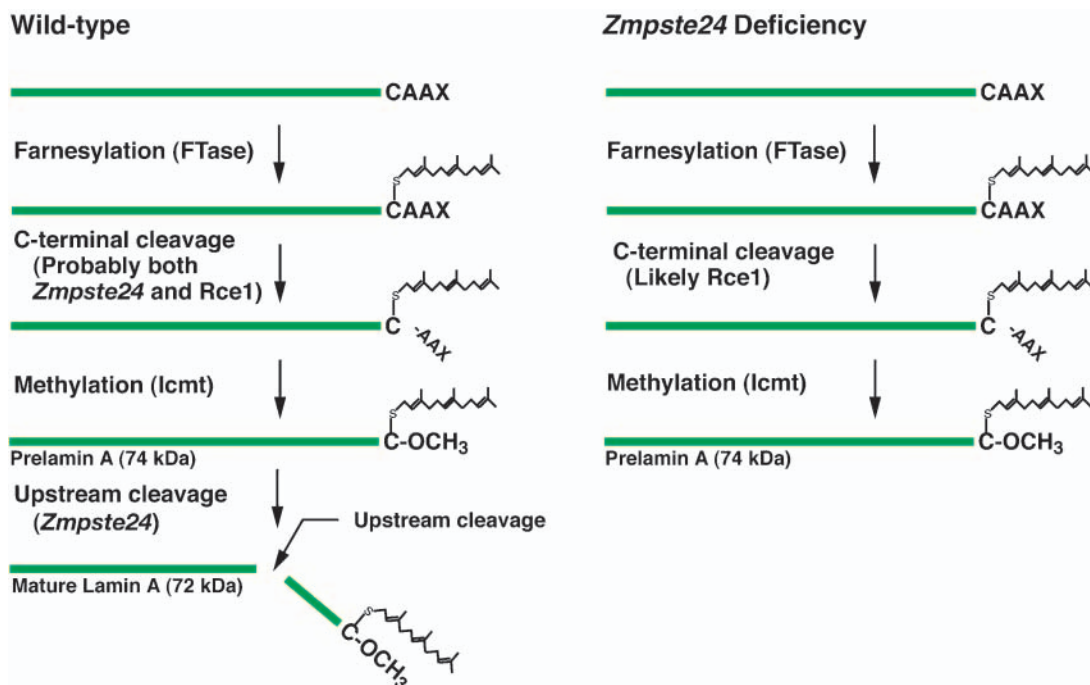


Fig. 9. Biogenesis of lamin A in normal cells and the failure to generate mature lamin A in the setting of *Zmpste24* deficiency. Left: Formation of lamin A from prelamins A in wild-type cells. Prelamin A (664 amino acids) undergoes four posttranslational processing steps. First, the cysteine of the CAAX motif is farnesylated by FTase. Second, the AAX is released. Third, the newly exposed farnesylcysteine is methylated. Fourth, the C-terminal 15 amino acids, including the farnesylcysteine methyl ester, are clipped off (by *Zmpste24*) and then degraded, leaving mature lamin A (646 amino acids). Right: Defective prelamins A processing in the setting of *Zmpste24* deficiency. By analogy to α -factor biogenesis in yeast (18–20, 47), we suspect that the AAX is probably released by Rce1 in *Zmpste24*^{−/−} cells. Another reason to suspect that Rce1 could release the AAX is the observation that Rce1 cleaves the AAX from lamin B1 (63). Blocking farnesylation with a farnesyltransferase inhibitor (FTI) would mean that the C terminus of progerin would terminate with an α -carboxylate anion rather than a farnesylcysteine methyl ester; this change would reduce the hydrophobicity of the C terminus of the protein (67) and would be expected to reduce the avidity of the molecule for the inner nuclear membrane and possibly influence its interactions with other nuclear proteins.

ability of lamin C to reach the nuclear envelope is at least partially dependent on lamin A (89).

Why does nature go to the trouble of modifying the C terminus of prelamins A, given that this portion of the molecule is simply clipped off and degraded? The most obvious explanation is that each of the posttranslational modifications render the C terminus of CAAX proteins more hydrophobic, facilitating the initial targeting of the protein to the inner nuclear membrane (81, 90, 91). Several

groups have evaluated mutant prelamins A constructs lacking the last 18 amino acids of the protein (i.e., “mature lamin A” constructs). These constructs are defective in their ability to be targeted to the nuclear envelope (88).

LAMIN A AND LAMIN C ARE ASSOCIATED WITH MULTIPLE GENETIC DISEASES

Lamins A and C have attracted great interest because *LMNA* mutations cause a host of different human genetic diseases (“laminopathies”), including Dunnigan-type familial partial lipodystrophy (FPLD) (92–94), Emery-Dreifuss muscular dystrophy (95), limb-girdle muscular dystrophy (78), familial cardiomyopathy with conduction system disease (96), one form of Charcot-Marie-Tooth peripheral neuropathy (97), and mandibuloacral dysplasia (MAD) (98). In addition, *LMNA* mutations cause the classic human progeroid syndrome Hutchinson-Gilford progeria syndrome (HGPS) (15) and also atypical Werner’s syndrome, a less severe progeroid syndrome that develops somewhat later in life (99, 100). Most but not all of the laminopathies are dominantly inherited; most are also caused by missense mutations, although HGPS is caused by a splicing mutation (15) and a nonsense mutation in codon 6 of lamin A/C causes Emery-Dreifuss muscular dystrophy (95).

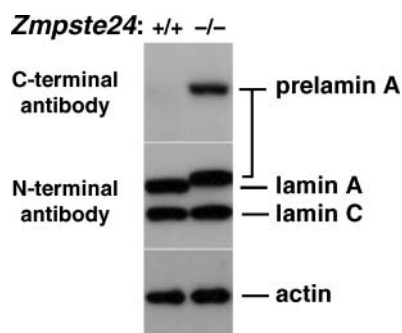


Fig. 10. Western blots of extracts from wild-type and *Zmpste24*^{−/−} fibroblasts with a C-terminal prelamins A antibody and an N-terminal lamin A/C antibody. Reproduced, with permission, from *The Proceedings of the National Academy of Sciences USA* (16).

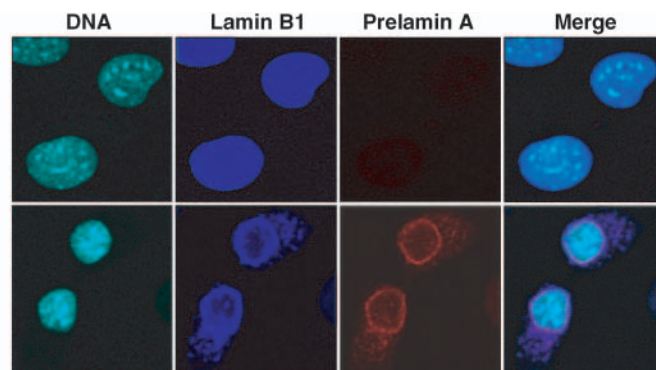


Fig. 11. Accumulation of prelamins A at the nuclear envelope in *Zmpste24*^{-/-} fibroblasts, as judged by confocal immunofluorescence microscopy. Normally, prelamins A is undetectable in cells; in the setting of *Zmpste24* deficiency, abundant prelamins A is located at the nuclear envelope, and blebs are evident.

FPLD is characterized by loss of adipose tissue in the extremities after puberty, increased adipose tissue in the neck and face, increased fasting and postprandial insulin levels, acanthosis nigricans, hypertriglyceridemia, reduced insulin-mediated glucose disposal, frank diabetes mellitus after age 20, and a heightened susceptibility to coronary artery disease (92, 93). Most of the mutations causing FPLD are located in exon 8, which encodes a portion of the C-terminal globular domain shared by lamins A and C (101). Crystallographic studies have revealed that most FPLD mutations are confined to a small region on the surface of the C-terminal globular domain of lamin A/C, whereas mutations causing muscular dystrophy are located throughout the lamin A/C protein core and its surface (101). Very similar findings were observed by Krimm et al. (102), who investigated lamin A/C structure by nuclear magnetic resonance. FPLD is not the only laminopathy characterized by loss of adipose tissue; this phenotype is also a prominent feature of MAD and HGPS.

Several laminopathies exhibit a recessive inheritance pattern. Homozygosity for a *LMNA* R298C mutation causes some cases of Charcot-Marie-Tooth neuropathy type IIA (97), a motor and sensory neuropathy characterized by muscle weakness, secondary foot deformities, a slight reduction in nerve conduction velocities, with the loss of large myelinated fibers and axonal degeneration. MAD is caused by homozygosity for R527H (98) or A529V substitutions (103). MAD is a progeroid syndrome characterized by postnatal growth retardation, lipodystrophy, insulin resistance, stiff joints, alopecia, abnormalities in the cranial sutures, osteolysis of the digits, shortening of the clavicle, micrognathia, and reduced ossification of alveolar bone.

Some but not all lamin A/C missense mutations cause abnormalities in the shape and structure of the nuclear envelope, resulting in misshapen nuclei (104). However, the mechanisms by which the lamin A/C mutations cause such a diverse collection of human diseases remain fairly mysterious. Presumably, the explanation relates to abnormalities in heterochromatin organization, the binding of nuclear factors and transcription factors (105), and secondary effects on gene expression (12, 78, 106). It has been

commonly suggested that muscle and heart disease with lamin A/C mutations could be attributable to the motion-related fragility of the nuclear envelope (12, 78, 106). Recently, Lammerding and coworkers (107) as well as Broers et al. (108) reported data in support of this concept. Lammerding et al. (107) used microscopic measurements and custom-built cell strain devices to demonstrate that lamin A/C knockout fibroblasts (*Lmna*^{-/-}) have impaired nuclear mechanics and mechanotransduction properties (107). The nuclei from *Lmna*^{-/-} fibroblasts exhibited exaggerated nuclear deformations, compared with *Lmna*^{+/+} control fibroblasts, when subjected to biaxial strain. Also, the nuclear envelope in *Lmna*^{-/-} fibroblasts was unequivocally more fragile than in *Lmna*^{+/+} fibroblasts, as judged by experiments in which a 70 kDa dextran was microinjected into cell nuclei. Perhaps most intriguingly, the *Lmna*^{-/-} fibroblasts exhibited significantly more cell death than *Lmna*^{+/+} fibroblasts when subjected to prolonged cyclic biaxial strain (107). Dual labeling with propidium iodide and an FITC-conjugated annexin V antibody revealed that the decrease in cell viability was caused by increased numbers of both necrotic and apoptotic cells. Lammerding et al. (107) also found diminished expression of the mechanosensitive genes *egr-1* and the antiapoptotic gene *iex-1* in *Lmna*^{-/-} fibroblasts in response to mechanical stimulation.

To date, no mutations in lamin B1 or lamin B2 have been linked to human disease, but it would not be particularly surprising if such associations were eventually identified. Vergnes and coworkers (109) characterized mice lacking a functional lamin B1 (*Lmnb1*^{-/-}). Homozygous *Lmnb1*^{-/-} mice survived embryonic development but died at birth with defects in lung and bone. Of note, *Lmnb1*^{-/-} fibroblasts displayed grossly misshapen nuclei, impaired differentiation, increased polyploidy, and premature senescence (109).

LAMIN A/C KNOCKOUT MICE

Although *Lmnb1* is expressed in all cells, *Lmna* is expressed late in development and then only in differenti-

ated cells (12, 110). This interesting expression pattern prompted Sullivan and coworkers (110) in the laboratory of Dr. Colin Stewart to generate *Lmna*^{-/-} mice. *Lmna*^{-/-} mice survive for ~5–6 weeks but then succumb with prominent signs of muscular dystrophy (110). Microscopic analysis of sections of *Lmna*^{-/-} muscle revealed small dystrophic myocytes, with “hyalin or flocculent cytoplasm,” and some myocyte apoptosis/necrosis (97). Also, the peripheral nerves of lamin A/C knockout mice are abnormal, with a reduction in axon density, an increase in axon diameter, and an increase in the number of nonmyelinated axons (97). *Lmna*^{-/-} mice have reduced subcutaneous fat, but this could be attributable to stress or reduced nutrition rather than to a bona fide lipodystrophy, as they had no apparent abnormalities in insulin, glucose, or triglyceride metabolism (110, 111). The absence of lamin A/C caused grossly misshapen nuclei and structurally abnormal nuclear envelopes, both in liver cells and in cultured fibroblasts (97).

An intriguing finding was that emerin, a nuclear envelope protein that binds to lamins A/C, was mislocalized to the ER in *Lmna*^{-/-} fibroblasts, indicating that lamin A or C (or both) is required for its proper targeting to the nuclear envelope (110). Emerin is important for muscle physiology; the emerin gene is mutated in X-linked Emery-Dreifuss muscular dystrophy (13). One group has reported that lamin A, but not lamin C, plays a key role in the targeting of emerin to the nuclear envelope (112). However, a group in France transfected both lamin A and lamin C cDNA constructs into lamin A/C-deficient fibroblasts, and they concluded that both lamin A and lamin C were capable of promoting the targeting of emerin to the nuclear envelope (113). They also showed that another integral membrane protein, nesprin-1 α , is also mislocalized to the ER in the absence of lamin A/C (113).

PROCESSING OF PRELAMIN A

Protein sequencing of the C-terminal region of lamin A indicated that prelamen A must undergo endoproteolytic processing, with the release of the farnesylcysteine methyl ester (114). Sinensky and coworkers (87) showed that the processing of prelamen A to lamin A is completely dependent on protein prenylation. The same group has also actively investigated the enzymatic activity responsible for clipping off the last 15 amino acids from farnesyl-prelamin A (82). They developed an assay for the endoprotease with a peptide substrate corresponding to the last 18 amino acids of the protein (ending with the methylated farnesylcysteine) (82). They found that the prelamen A endoprotease was present in crude nuclear extracts and that the enzyme was entirely specific for a prelamen A peptide containing an S-farnesylated cysteine methyl ester (82). The endoprotease was inhibited by N-acetyl farnesylcysteine, and the removal of the methyl ester from the substrate reduced enzymatic activity (82). Inhibitor studies suggested that the prelamen A endoprotease activity may have been a serine protease (82, 91). Dr. Sinensky's laboratory has

developed several lines of evidence indicating that the biochemical activity is located in the nucleus (82, 91), and this concept has been supported by others (88).

In yeast, a-factor is cleaved twice by Ste24p (17, 19). Simply because prelamen A in mammals is also cleaved twice, we hypothesized that prelamen A might be a substrate for Zmpste24 (9, 47). At the time, this hypothesis seemed extremely far-fetched, given that prelamen A had no obvious structural similarities to yeast a-factor. In any case, to approach this issue experimentally, we generated *Zmpste24*^{-/-} mice (54). Along with another group that also generated *Zmpste24*^{-/-} mice (83), we showed that *Zmpste24*^{-/-} fibroblasts manifested a striking defect in prelamen A processing (54), with an accumulation of prelamen A and a complete absence of mature lamin A (Fig. 10). With an antibody specific for the C terminus of prelamen A (the segment of prelamen A that is normally cleaved off), we observed a striking accumulation of a 74 kDa prelamen A in *Zmpste24*^{-/-} cells. In extracts from wild-type cells, prelamen A is virtually undetectable, for the simple reason that processing of prelamen A to mature lamin A is an extremely efficient process, rapidly converting the prelamen A to mature lamin A. Western blots of *Zmpste24*^{-/-} extracts with an antibody against the N terminus of lamin A/C revealed lamin C and prelamen A (74 kDa) but absolutely no mature lamin A.

An FTI completely blocked the processing of prelamen A to mature lamin A (79), a result that was consistent with earlier studies from the laboratory of Sinensky (87). We also asked whether prelamen A might accumulate in fibroblasts lacking *Icmt* (62) or *Rce1* (35). In our initial experiments with *Icmt*^{-/-} fibroblasts, prelamen A processing appeared to be fully blocked. That result was consistent with the earlier biochemical studies from Sinensky and colleagues (82) indicating that the C-terminal methyl ester was essential for the endoproteolytic processing reaction. However, our recent experiments with several immortalized *Icmt*^{-/-} cell lines have shown that the defect in prelamen A processing is only partial (115). We invariably observe an increase in the amount of prelamen A in *Icmt*^{-/-} cell lines, as judged by Western blots with an antibody against the C terminus of prelamen A (Fig. 12). Thus, the prelamen A processing in *Icmt*^{-/-} fibroblasts is clearly abnormal. However, when Western blotting is performed with an antibody against the N-terminal portion of lamin A/C, we always observe some mature lamin A. Thus, *Icmt* deficiency causes a partial but not a complete blockade in the processing of prelamen A to mature lamin A.

Prelamen A processing in *Rce1*^{-/-} fibroblasts was normal (79). One interpretation of this finding is that *Rce1* plays absolutely no role in prelamen A processing (59). However, we believe that this interpretation is unlikely. In yeast, the cleavage of the AAX from a-factor is a redundant function of *Rce1p* and *Ste24p* (17, 19, 47), and we suspect that both *Rce1* and *Zmpste24* play redundant roles in cleaving the AAX from prelamen A (79). No proof for this view yet exists, but several “soft” observations tend to support it. First, *Rce1* processes a very broad range of mammalian CAAX proteins (35, 58), and there is no rea-

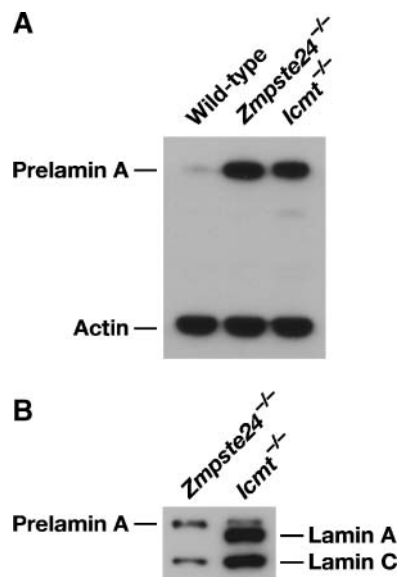


Fig. 12. Increased amounts of prelamin A in fibroblasts lacking *Icm1*. A: Western blot of wild-type, *Zmpste24*^{-/-}, and *Icm1*^{-/-} fibroblasts with a prelamin A-specific antibody and an antibody against β-actin. B: Western blot of *Zmpste24*^{-/-} and *Icm1*^{-/-} fibroblasts with a lamin A/C-specific antibody. Reproduced, with permission, from *The Enzymes* (115).

son to believe that it would not be capable of cleaving prelamin A. Rce1 is exclusively responsible for cleaving the AAX from another lamin, lamin B1 (63), in which the CAAX motif (CAIM) is similar to that in prelamin A (CSIM). Second, the prelamin A CAAX motif is actually a better substrate for yeast Rce1p than yeast Ste24p (Fig. 5), and the specificities of the mouse *Zmpste24* enzymes resemble those of yeast Ste24p (54).

The precise biochemical role of *Zmpste24* in prelamin A processing is beginning to come into focus. Corrigan and coworkers (81) have presented evidence that recombinant ZMPSTE24, produced in insect cells, is capable of carrying out both the release of the AAX from a short prelamin A peptide and the release of the 15 additional amino acids. The ability of *Zmpste24* to clip the AAX from prelamin A parallels the ability of Ste24p to cleave the AAX from *a*-factor (20). However, we suspect that *Zmpste24*'s ability to act as a CAAX endoprotease beyond prelamin A is very restricted. We tested whether recombinant *Zmpste24* would be capable of processing some or all of the CAAX protein substrates that accumulate in *Rce1*^{-/-} fibroblasts (54). Whole cell extracts from *Rce1*^{+/+} and *Rce1*^{-/-} fibroblasts were incubated with recombinant *Icm1*, Sadenosyl-L-[methyl-¹⁴C]methionine, and either recombinant mouse Rce1 or *Zmpste24*. We noted significantly increased carboxyl methylation when recombinant Rce1 was added to extracts from *Rce1*^{-/-} fibroblasts, reflecting the processing of accumulated Rce1 substrates (54). No such increase was observed when recombinant *Zmpste24* was added to extracts from *Rce1*^{-/-} fibroblasts (54), indicating that *Zmpste24* has little if any ability to process the substrates that accumulate in *Rce1*^{-/-} fibroblasts.

Zmpste24^{-/-} cells contain a striking accumulation of prelamin A. One would expect that prelamin A would be farnesylated in *Zmpste24*^{-/-} cells, because farnesylation precedes the endoproteolytic cleavage step mediated by *Zmpste24*. Indeed, several lines of evidence suggest that it actually is farnesylated. First, the electrophoretic migration of prelamin A in human and mouse *Zmpste24*^{-/-} fibroblasts is retarded when cells are grown in the presence of an FTI (116). Also, the prelamin A in *Zmpste24*^{-/-} fibroblasts is located at the nuclear envelope (Fig. 11) (16, 83, 117), whereas nonfarnesylated prelamin A is misdirected to the nucleoplasm (117).

As explained in more detail below, FTIs have recently been used to improve the nuclear shape in progeroid disorders characterized by an accumulation of farnesylated prelamin A at the nuclear envelope (116, 117). The rationale is that inhibition of farnesylation would mislocalize farnesyl-prelamin A away from the nuclear envelope, thereby attacking the presumptive cause of the misshapen nuclei. However, we suggest that this may not be the only pharmacological strategy. As noted previously, methylation appears to be critical for the membrane attachment of farnesylated proteins (36, 67), and we would not be surprised if *Icm1* inhibitors, currently under development (68–70), might work independently or synergistically to mislocalize farnesyl-prelamin A within the nucleus.

ZMPSTE24 KNOCKOUT MICE

Mice lacking *Zmpste24*, initially developed by Leung and coworkers (54), develop a host of disease phenotypes. Before creating a knockout mouse, we cloned the mouse *Zmpste24* cDNA and gene (54). The mouse and human amino acid sequences were 93% identical and were 36% identical to the *S. cerevisiae* Ste24p. To assess the integrity of the *Zmpste24* cDNA clone, we tested its ability to complement the *a*-factor production defect in *ste24Δrce1Δ* yeast. As judged by a standard halo assay, mouse *Zmpste24* restored *a*-factor production (Fig. 13A) (54). A mutant *Zmpste24* lacking the HEXXH zinc metalloproteinase motif was incapable of processing yeast *a*-factor (Fig. 13A) (54). The specificities of mouse *Zmpste24* mirrored those of yeast Ste24p; mouse *Zmpste24* processed wild-type *a*-factor and a mutant *a*-factor terminating in CAMQ, but not *a*-factor terminating in CTLM (54).

To inactivate *Zmpste24* in mice, we used a targeting vector to replace the exon encoding the HEXXH motif with a floxed *neo* (54). Once mice were in hand, we determined whether the targeted mutation actually abolished *Zmpste24* enzymatic activity. As expected, no enzymatic activity was detectable. Membranes from *Zmpste24*^{-/-} fibroblasts and tissues were completely incapable of producing mature *a*-factor from a mutant 15-mer *a*-factor peptide that terminated in CAMQ (i.e., a substrate specific for Ste24p and *Zmpste24*) (54). In addition, we tested the ability of membranes from *Zmpste24*^{-/-} and *Zmpste24*^{+/+} fibroblasts and tissues to cleave the N terminus from the P1 form of *a*-factor (converting it to the shorter *a*-factor intermediate P2).

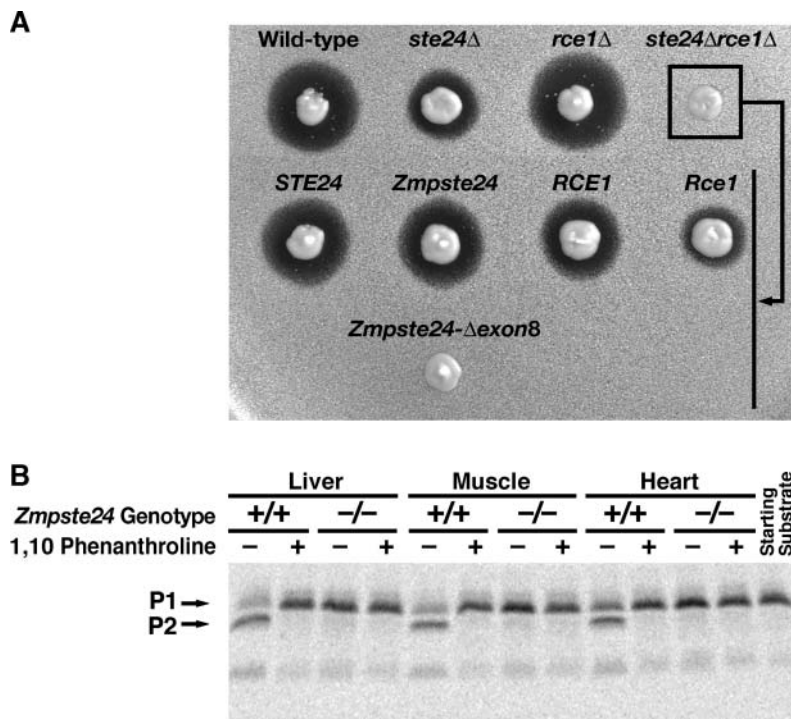


Fig. 13. A: Yeast halo assay demonstrating that the expression of yeast *RCE1*, mouse *Rce1*, yeast *STE24*, and mouse *Zmpste24* restores the production of *a*-factor in *ste24Δrce1Δ* yeast. A mutant mouse *Zmpste24* construct lacking exon 8 sequences (which encode the HEXXH motif) did not restore *a*-factor production. B: Reduced ability of membranes from *Zmpste24*^{-/-} tissues to carry out the N-terminal processing of *a*-factor. A ³⁵S-labeled P1 *a*-factor intermediate was prepared from a yeast strain that lacked *STE24* and expressed *MFA1* from a high-copy plasmid. Proteolysis reactions were performed by incubating the radiolabeled P1 with mouse membranes for 2 h at 30°C in the absence or presence of 1,10-phenanthroline. The *a*-factor intermediates were then immunoprecipitated with an *a*-factor-specific antiserum and size-fractionated by SDS-PAGE. Dried gels were analyzed by autoradiography and with a phosphor imager. The N-terminal processing reaction cleaves seven amino acids from the N terminus of P1, yielding the shorter intermediate. Reproduced, with permission, from *The Journal of Biological Chemistry* (54).

Crude membranes from *Zmpste24*^{+/+} ES cells and tissues readily converted P1 to P2, whereas membranes from *Zmpste24*^{-/-} cells and tissues did not (Fig. 13B).

Zmpste24^{-/-} mice develop a host of disease phenotypes consistent with features of human progeria and human laminopathies. *Zmpste24*^{-/-} mice weigh slightly less than their littermates at weaning and gain weight slowly. By 4 months of age, the mice develop long, thin, and discolored lower incisors and kyphosis of the spine, and some begin to lose hair (Fig. 14). Two additional phenotypes of *Zmpste24* deficiency are obvious: bone disease and muscle weakness. These phenotypes are progressive, and the mice either die or need to be euthanized by 6–7 months of age. By ~20 weeks of age, nearly every rib in *Zmpste24*^{-/-} mice is broken in the vicinity of the costovertebral junction, obvious from hypertrophic calluses at the fracture sites (Fig. 15).

Microscopic sections also revealed that the broken ribs were surrounded by exuberant fibrous tissue (Fig. 15). The fracture sites were surprisingly acellular, with minimal

evidence of healing. *Zmpste24*^{-/-} mice had fractures or osteolytic lesions in multiple other locations, including the scapula, clavicle, sternum, zygomatic arch, mandible, and humerus. By 8 weeks of age, 100% of *Zmpste24*^{-/-} mice had osteolytic lesions in the posterior portion of the zygomatic arch (Fig. 16). Microcomputed tomography (μCT) scans of 2–3 month old mice also revealed striking micrognathia and a peculiar reduction in the zigzag appearance of the cranial sutures (Fig. 16). Quantitative analysis of μCT scans revealed that thoracic vertebrae of 3 month old *Zmpste24*^{-/-} mice had reduced bone density (79). Interestingly, the bone density was entirely normal at 3 weeks of age, as judged by μCT scans.

Zmpste24^{-/-} mice did not manifest evidence of increased bone turnover. Urinary levels of deoxypyridinoline, a bone collagen breakdown product (118), were no different in *Zmpste24*^{-/-} and *Zmpste24*^{+/+} mice. Also, bones from *Zmpste24*^{-/-} and *Zmpste24*^{+/+} mice contained similar numbers of osteoclasts, as judged by staining for tartrate-resistant acid phosphatase (79). The plasma levels of calcium

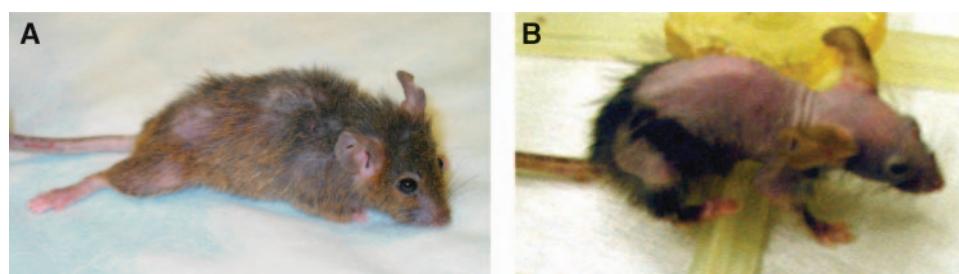


Fig. 14. Photographs of *Zmpste24*^{-/-} mice. A: A *Zmpste24*^{-/-} mouse showing loss of fur and the characteristic dragging of a hind limb. B: Loss of fur and subcutaneous fat in a 6 month old *Zmpste24*^{-/-} mouse. A is reproduced, with permission, from *The Proceedings of the National Academy of Sciences USA* (79).

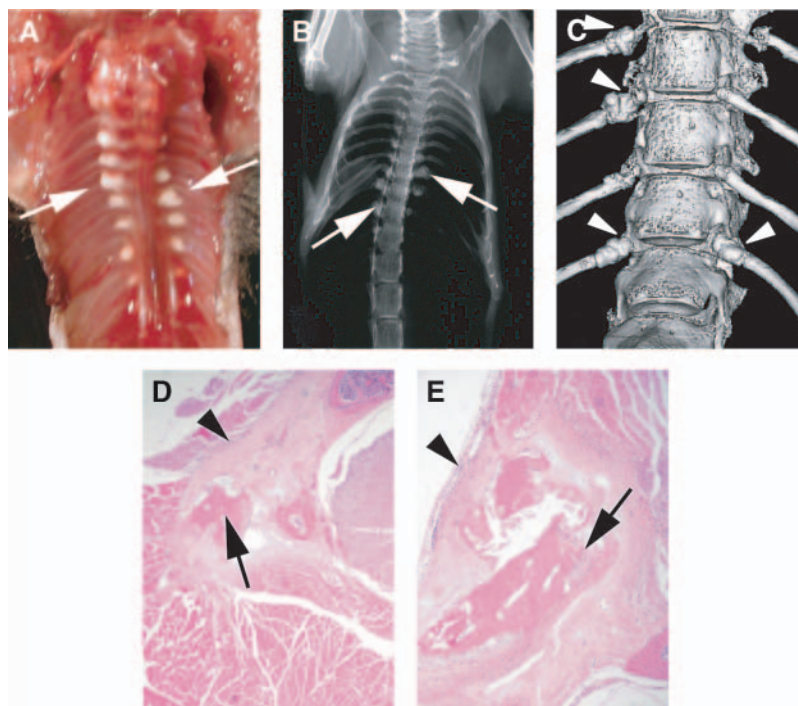


Fig. 15. Rib fractures in a 24 week old *Zmpste24*^{-/-} mouse. A: Thorax after removal of the heart and lungs. Fibrotic lesions surrounding broken ribs are indicated by arrows. B: Radiograph of a *Zmpste24*^{-/-} mouse, revealing callus formation surrounding rib fractures (arrows). C: Surface rendering of a microcomputed tomography (μCT) scan of the lower thoracic spine of a *Zmpste24*^{-/-} mouse. Callus is visible at the tips of several ribs near the costovertebral joints (arrowheads). D, E: Hematoxylin and eosin-stained sections of rib fractures (arrows) and surrounding fibrosis (arrowheads). Reproduced, with permission, from *The Proceedings of the National Academy of Sciences USA* (79).

and phosphate were normal in the *Zmpste24*^{-/-} mice, and these animals did not have increased plasma levels of alkaline phosphatase (79).

All of the bone abnormalities in *Zmpste24*^{-/-} mice were age-related in that they were completely undetectable at 3 weeks of age but extremely obvious by 3 months of age. It seems likely that the bone disease in *Zmpste24*^{-/-} mice is attributable to the development of unhealthy osteoblasts, which might reasonably be expected to cause osteoporosis, osteolytic lesions, and poorly healing fractures. We examined osteoblasts from the 12th thoracic vertebrae of 3 month old *Zmpste24*^{-/-} mice by transmission electron microscopy. We found numerous sick, vacuolated osteoblasts in *Zmpste24*^{-/-} bone, devoid of the usual sheets of rough ER that characterize wild-type osteoblasts (Fig. 17).

Zmpste24^{-/-} mice exhibit a slow, hobbling gait, frequently dragging their hind limbs (Fig. 14A). In addition, *Zmpste24*^{-/-} mice were markedly deficient in their ability to hang onto a grid after it was turned upside down, whereas wild-type mice hung on almost indefinitely. This phenotype was also identified in *Lmna*^{-/-} mice (110). In *Lmna*^{-/-} mice, skeletal muscle pathology was easily detectable. However, even with the help of skilled pathologists, we could not find abnormalities in hematoxylin and eosin-stained sections of skeletal muscle from *Zmpste24*^{-/-} mice at any age (79). It is quite possible that more sophisticated histological studies could reveal a muscular dystrophy. Alternatively, perhaps there is a neuropathy akin to that in

Lmna^{-/-} mice and humans with the R298C *LMNA* mutation (97). Further neuromuscular studies in *Zmpste24*^{-/-} mice are needed.

In analyzing the *Zmpste24*^{-/-} mice, the muscular dystrophy-like phenotypes made sense, inasmuch as a variety of lamin A/C missense mutations cause muscular dystrophy (95). However, the bone phenotypes were perplexing (79), because no association of lamin A/C mutations and bone disease had yet been described. Moreover, a collagen gene, *Col9a2*, is located only a few kilobases from *Zmpste24*, and we were initially worried that the bone phenotypes in the *Zmpste24*^{-/-} mice could have been caused by a remote effect of the PGK-*neo* on *Col9a2* expression (79). Over the next few years, however, a variety of considerations led us to suspect that the bone disease in *Zmpste24*^{-/-} mice was in fact caused by the prelamin A processing defect. First, we found that the expression of *Col9a2* was not perturbed in *Zmpste24*^{-/-} mice (harboring the PGK-*neo*) (79). Second, the bone phenotypes were unaltered in *Zmpste24*^{-/-} mice in which the PGK-*neo* had been removed by Cre-mediated recombination (79). Third, an association between lamin A/C mutations and MAD was discovered by Novelli and coworkers (98), and humans with MAD and mice with *Zmpste24* deficiency exhibited many similar phenotypes, including retarded growth, reduced subcutaneous fat, alopecia, osteoporosis, micrognathia, abnormalities of the cranial sutures, and osteolysis of multiple bones, including the clavicle. Fourth, Mounkes et al. (119) charac-

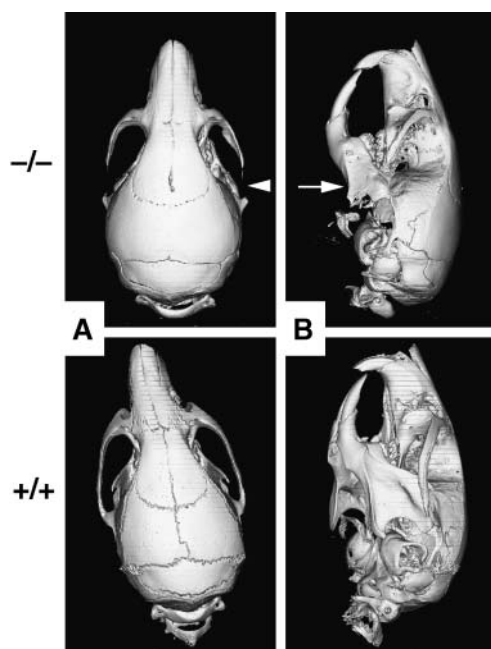


Fig. 16. μ CT scans illustrating bony lesions in *Zmpste24*^{-/-} mice. Shown are surface renderings of top (A) and lateral (B) surfaces of the skulls of 8 week old *Zmpste24*^{-/-} and *Zmpste24*^{+/+} mice. The arrowhead in panel A shows an osteolytic lesion in the zygomatic arch. The arrow in panel B indicates a small mandible. Reproduced, with permission, from *The Proceedings of the National Academy of Sciences USA* (79).

terized mice with a lamin A/C missense mutation (L530P) and multiple mRNA splicing abnormalities; those mice had incisor and bone phenotypes very similar to those in *Zmpste24*^{-/-} mice.

Another group also produced *Zmpste24*^{-/-} mice (83) by replacing exons 2 and 3 with a β geo cassette and observed many of the same abnormalities found in our *Zmpste24*^{-/-} mice (slow growth, early death, loss of fur, kyphosis, abnormal gait, muscle weakness, and abnormal prelamin A

processing). However, they did not report the micrognathia, osteolytic lesions in the zygomatic arch, osteoporosis, or bone fracture phenotypes. They reported that their mice developed myocardial fibrosis and heart failure, phenotypes that we have never observed, even in very old *Zmpste24*^{-/-} mice. They also found reduced adipose tissue in *Zmpste24*^{-/-} mice and concluded that the mice had a lamin A-related partial lipodystrophy (83). We observed reduced fat stores but concluded that this phenotype could have been attributable in part to the bone abnormalities (i.e., micrognathia and complete destruction of the zygomatic arch) (79). The different strains of knockout mice have not yet been examined side by side, but subtle differences in knockout mice produced by different groups is common (120), potentially resulting from genetic strain differences and the precise nature of the underlying knockout mutation.

ZMPSTE24 DEFICIENCY CAUSES MISSHAPEN NUCLEI AND CELL GROWTH ABNORMALITIES

As noted previously, farnesyl-prelamin A accumulates at the nuclear envelopes of *Zmpste24*^{-/-} fibroblasts (16, 83). This accumulation is associated with the development of misshapen nuclei (16, 83). In one of our initial experiments, we compared the shape of nuclei in *Zmpste24*^{+/+} and *Zmpste24*^{-/-} fibroblasts and found that nuclear blebbing was more common in the *Zmpste24*^{-/-} cells (19% vs. 8% in *Zmpste24*^{+/+} fibroblasts; $P < 0.0001$). However, we have found that the percentage of misshapen nuclei in *Zmpste24*^{-/-} fibroblasts can vary substantially, so good experimental controls are essential. In some experiments with very early-passage primary *Zmpste24*^{-/-} fibroblasts, we observed no increase in misshapen nuclei compared with wild-type control fibroblasts. However, in some immortalized *Zmpste24*^{-/-} fibroblast cell lines, nearly 60% of cells have grossly misshapen nuclei.

A key question is how the misshapen nuclei affect, or at least correlate with, gene expression and the growth characteristics of cells. We have generated multiple independent lines of primary *Zmpste24*^{-/-} and *Zmpste24*^{+/+} embryonic fibroblasts and carefully examined their growth characteristics over five to six passages with sensitive growth assays and have not observed significant differences in growth rates. Similarly, *Zmpste24*^{-/-} and *Zmpste24*^{+/+} ES cell lines had similar rates of growth in vitro (54), but that is perhaps not surprising because *Lmna* is expressed at low levels in those cells. *Zmpste24*^{-/-} ES cells were quite efficient in populating multiple tissues of chimeric mice, suggesting that the accumulation of prelamin A did not have large consequences on cell growth in the early phases of development (54). However, it is quite possible that these relatively short-term experiments in primary fibroblasts (and in ES cells) overlooked a significant effect of the *Zmpste24* mutation on cell growth later in life. Along these lines, Mounkes and colleagues (119) generated a mouse expressing a mutant form of lamin A/C (associated with alternative splicing within *Lmna*) and observed premature

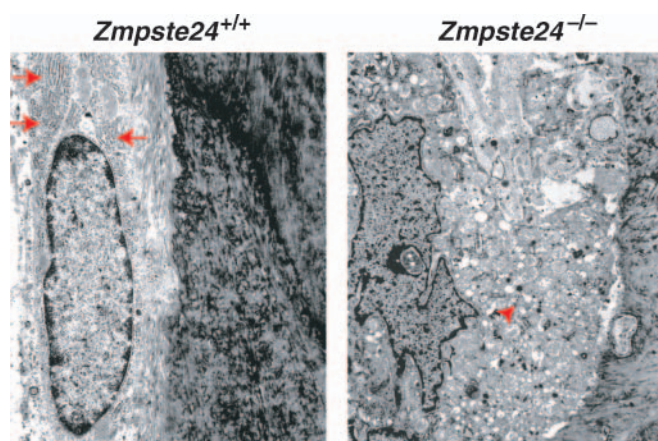


Fig. 17. Abnormal osteoblasts from a 4 month old *Zmpste24*^{-/-} mouse. Left: In wild-type osteoblasts, sheets of rough endoplasmic reticulum (ER) are visible (red arrows). Right: *Zmpste24*^{-/-} osteoblasts appear abnormal, with vacuolated cytoplasm (red arrowhead) and markedly reduced amounts of rough ER.

senescence and slow growth in fibroblasts harvested from the tissues of older mice. Recently, similar findings were reported in *Zmpste24*^{-/-} mice (121).

STRIKING EVIDENCE FOR THE TOXICITY OF FARNESYL-PRELAMIN A

We reasoned that the most parsimonious explanation for both the cellular and “whole animal” phenotypes in *Zmpste24*^{-/-} mice was the “toxicity” of farnesyl-prelamin A. However, a skeptic could have easily argued that many of the *Zmpste24* phenotypes are fairly nonspecific and might have been caused by the failure to cleave another, as-yet-unidentified *Zmpste24* substrate (aside from prelam A) (79). To test the idea that the phenotypes were indeed caused by the toxicity of farnesyl-prelamin A, we performed a simple genetic experiment. We reasoned that if the disease phenotypes were truly caused by prelam A, then they should be ameliorated by reducing the synthesis of prelam A (16).

To test this concept, Fong et al. (16) compared the phenotypes of *Zmpste24*^{-/-} mice and littermate *Zmpste24*^{-/-} mice bearing one *Lmna* knockout allele (*Zmpste24*^{-/-}*Lmna*^{+/-}) (16). As expected, Western blots revealed lower amounts of prelam A in *Zmpste24*^{-/-}*Lmna*^{+/-} fibroblasts than in *Zmpste24*^{-/-} fibroblasts (Fig. 18). The results of this genetic experiment were striking and unequivocal: the *Zmpste24*^{-/-}*Lmna*^{+/-} mice were completely protected from all disease phenotypes. The growth rate and muscle strength of the *Zmpste24*^{-/-}*Lmna*^{+/-} mice were entirely normal, and the mice had absolutely no bone disease (Fig. 19) (16). These data strongly indicated that all of the recognized phenotypes in *Zmpste24*^{-/-} mice are attributable to defective lamin A biogenesis. Moreover, *Zmpste24*^{-/-}*Lmna*^{+/-} fibroblasts exhibited a significantly reduced frequency of misshapen nuclei (Fig. 20) (16). Thus, there was no “disconnect” between the disease phenotypes in mice and the frequency of misshapen nuclei in cultured cells. In other words, the elimination of blebbing at the cellular level appeared to be correlated with the elimination of progeria-like phenotypes at the whole animal level.

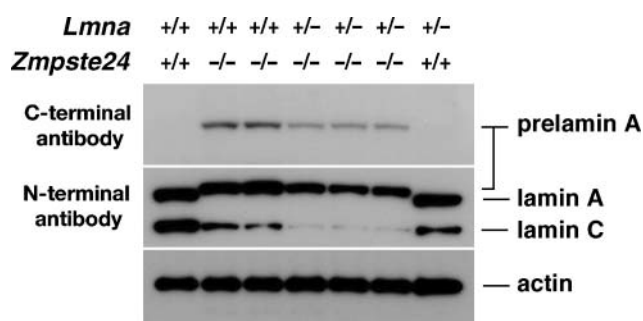


Fig. 18. Western blots of extracts from wild-type, *Zmpste24*^{-/-}, and *Zmpste24*^{-/-}*Lmna*^{+/-} fibroblasts with a C-terminal prelam A antibody and an N-terminal lamin A/C antibody. Reproduced, with permission, from *The Proceedings of the National Academy of Sciences USA* (16).

The fact that a single *Lmna* knockout allele caused such profound beneficial effects is remarkable because the *Zmpste24*^{-/-}*Lmna*^{+/-} fibroblasts also had reduced expression of lamin C. One could have persuasively argued that any mutation that reduced lamin C production might worsen nuclear shape and disease phenotypes rather than improve them (16). So why should heterozygous lamin A/C deficiency in *Zmpste24*^{-/-} mice ameliorate rather than worsen disease phenotypes? We proposed that the most likely explanation was that farnesyl-prelamin A is toxic to cells and that reducing the amount of prelam A synthesis by 50% decreases steady-state farnesyl-prelamin A levels below the threshold for toxicity (16).

Very recently, a group in Spain bred *Zmpste24*^{-/-}*Lmna*^{+/-} mice and found that heterozygosity for *Lmna* deficiency normalized the retarded growth phenotype in their line of *Zmpste24*^{-/-} mice (121). These studies were important because they confirmed the findings by Fong and coworkers (16) and reinforced the concept that the accumulation of prelam A underlies disease phenotypes.

HGPS

Interest in *Zmpste24*^{-/-} mice and their phenotypes increased considerably in 2003 with the finding that the classic genetic progeroid syndrome in humans, HGPS, is caused by the production of a mutant prelam A that is farnesylated but cannot be converted to mature lamin A (15). The accumulation of the mutant prelam A in HGPS cells leads to dramatically misshapen nuclei (15), paralleling the situation with *Zmpste24* deficiency. Also, humans with HGPS and *Zmpste24*^{-/-} mice have many phenotypes in common, including retarded growth, osteoporosis, alopecia, micrognathia, reduced subcutaneous fat, and osteolysis of the clavicle and other bones.

HGPS is extremely rare in humans, occurring in only 1 in 8 million births (15, 122). Individuals with HGPS appear normal at birth and remain so for 6–12 months, when the infant fails to gain weight and develops alopecia and sclerodermatous changes of the skin. Subcutaneous fat is generally reduced, and the scalp veins become prominent as subcutaneous fat and hair are lost. Affected children grow slowly and frequently weigh no more than 20 kg when fully grown. They have delayed dentition and multiple skeletal abnormalities, including micrognathia and osteoporosis. The average life expectancy for a patient with HGPS is 13 years, with ~90% of patients dying from progressive atherosclerosis of the coronary and cerebral arteries. In our view, the toll from atherosclerosis is unbelievably severe, a quantum leap in severity above the atherosclerotic disease in middle-aged FPLD patients, suggesting that the HGPS may cause unique pathology in the arterial wall. There are few histological descriptions of the arterial disease in HGPS (15, 122). However, Dr. Stephen Schwartz, a pathologist at the University of Washington, reviewed the topic of atherosclerosis in HGPS for a National Institutes of Health-sponsored HGPS workshop in

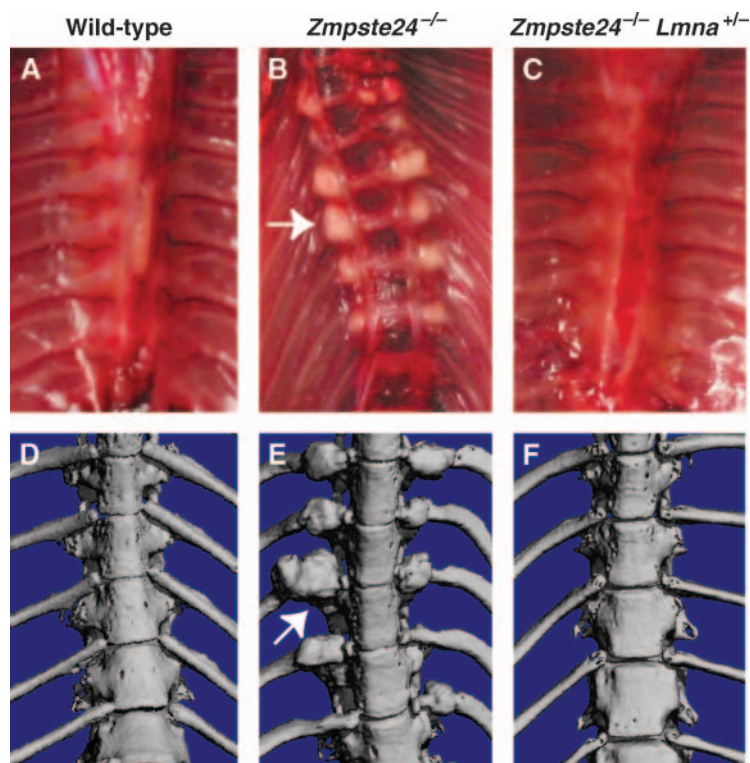


Fig. 19. Fractures of ribs near the costovertebral joint occur in *Zmpste24*^{-/-} mice but not in wild-type or *Zmpste24*^{-/-} *Lmna*^{+/-} mice. A–C: Photographs of the thorax after removal of the heart and lungs, revealing fracture callus in a *Zmpste24*^{-/-} mouse (in B, the arrow indicates callus around a rib fracture). D–F: Surface renderings of μ CT scans of the thoracic spine in 28 week old wild-type, *Zmpste24*^{-/-}, and *Zmpste24*^{-/-} *Lmna*^{+/-} mice. In the *Zmpste24*^{-/-} mouse (E), fracture callus is indicated by an arrow. Reproduced, with permission, from *The Proceedings of the National Academy of Sciences USA* (16).

July 2003, and he concluded that the plaques in HGPS are similar to those occurring in older adults (i.e., fibrous caps, lipid-filled macrophages, pools of extracellular lipid) (personal communication).

HGPS is often said to be a segmental aging syndrome, in that many of the classic features of human aging, such as senile dementia and an increased susceptibility to cancer, are absent. HGPS patients do not exhibit significant muscle weakness (54, 79, 83), unlike the situation with *Zmpste24*^{-/-} mice.

Identifying the genetic basis of HGPS was no easy feat, both because the disease is extremely rare and because all cases turned out to be caused by de novo mutations. However, in a tour de force, the genetic basis of HGPS was identified by Eriksson and coworkers (15). They localized the HGPS gene to chromosome 1q after observing two HGPS patients with uniparental isodisomy of 1q and one patient with a 6 Mb paternal 1q deletion. Sequencing of *LMNA*, which was located within this interval, revealed that 18 of 20 classic HGPS patients harbored the same de

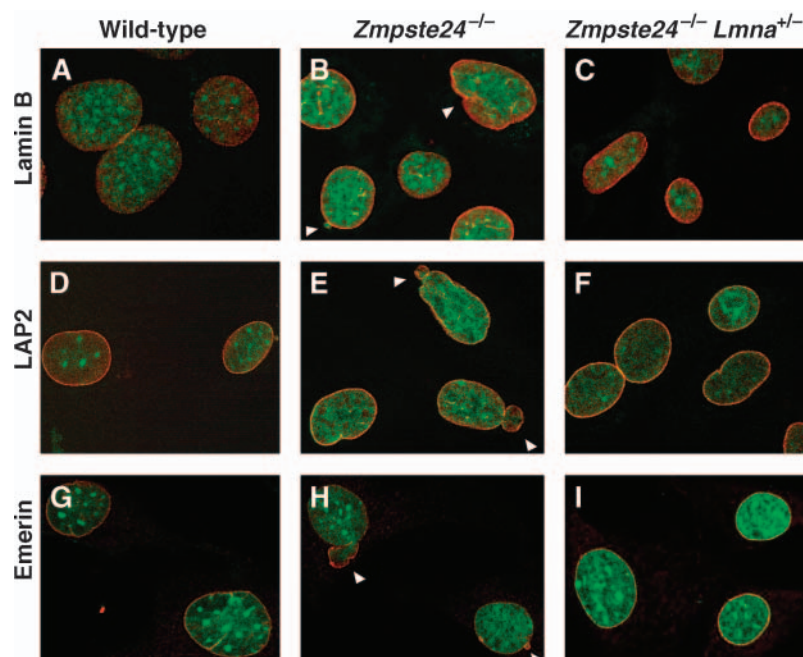


Fig. 20. Analysis of nuclear shape in wild-type, *Zmpste24*^{-/-}, and *Zmpste24*^{-/-} *Lmna*^{+/-} fibroblasts by laser-scanning fluorescence microscopy. The nuclear envelope was visualized with antibodies to lamin B (A–C), LAP2 (D–F), or emerin (G–I) (red), and DNA was visualized with SYTOX Green staining (green). Arrowheads indicate nuclear blebs. Quantification of blebbing revealed a highly significant reduction in blebs in *Zmpste24*^{-/-} *Lmna*^{+/-} fibroblasts (16). Reproduced, with permission, from *The Proceedings of the National Academy of Sciences USA* (16).

novo single base pair substitution in exon 11 (GGC to GGT, G608G). An additional HGPS patient had a different nucleotide substitution within the same codon. Both mutations activated a cryptic splice site within exon 11, causing an in-frame deletion of 50 amino acids in prelamin A (residues 607–656). The alternative splicing from mid-exon 11 to exon 12 was only partial; the mutant allele also yielded a full-length prelamin A transcript. The alternatively spliced message could easily be detected by RT-PCR, and a truncated prelamin A protein, now generally called progerin, could easily be detected by Western blotting, both in fibroblasts and in lymphoblasts (15). HGPS is a dominantly inherited disease, so patients have one normal allele producing lamin A and lamin C and one mutant allele producing lamin A, lamin C, and progerin. By SDS-PAGE, progerin migrates midway between lamin C and lamin A; the intensity of the progerin band in HGPS cells is typically approximately one-fifth to one-fourth of that of lamin C or mature lamin A.

Because the CAAX motif of prelamin A is encoded by exon 12, which is retained in the mutant HGPS transcript, progerin is expected to terminate with a CAAX motif and undergo all of the usual CAAX motif modifications (15). Importantly, however, the 50 amino acid deletion eliminates the site for the second endoproteolytic cleavage step, preventing the release of the farnesylcysteine methyl ester (Fig. 21).

The codon 608 mutation causing HGPS was also identified by Cao and Hegele (123); Hegele had earlier identified the association between *LMNA* mutations and Dunnigan-type FPLD (92, 93). A group in France also identified the codon 608 prelamin A mutation in a pair of HGPS pa-

tients and identified the aberrant mRNA splicing, but they did not detect a truncated prelamin A protein in cells (124). They also reported that wild-type lamin A was absent in at least some cases of HGPS and proposed that the mutant prelamin A in HGPS might prevent the “transcriptional processing” of the wild-type *LMNA* allele. There are no data to support this proposal, however, and studies of *LMNA* transcripts in HGPS cells by another group indicated that transcription from the wild-type *LMNA* gene is normal (125).

The synthesis of progerin results in striking abnormalities in nuclear shape (15), very much like the situation in *Zmpste24*^{-/-} fibroblasts (16, 83, 116). Experiments by Goldman et al. (126), involving microinjection of progerin as well as transfection experiments, revealed that progerin is normally targeted to the nuclear envelope and is entirely responsible for the misshapen nuclei. The fact that progerin is targeted to the nuclear envelope suggests that the protein is farnesylated; indeed, this concept has now been supported by several experimental observations. First, we showed that a highly specific FTI mislocalizes progerin away from the nuclear envelope to the nucleoplasm (117). Second, a specific FTI was recently shown to retard the electrophoretic mobility of progerin (127), just as these drugs retard the electrophoretic mobility of prelamin A in *Zmpste24*^{-/-} fibroblasts (116). Goldman and coworkers (126) concluded that HGPS cells also exhibit an accumulation of wild-type prelamin A at the nuclear envelope, as judged by immunofluorescence microscopy. However, no one, as far as we are aware, has ever documented an accumulation of wild-type prelamin A in HGPS cells by Western blot analysis.

HGPS fibroblasts grow slowly, and Goldman et al. (126) observed that the growth rate is markedly retarded with increased passage numbers. On the other hand, culturing cells clearly selects for more rapidly growing subpopulations of cells, and the results of genetic studies by Eriksson and coworkers (15) strongly suggested that somatic recombination events can occasionally rescue the slow-growth phenotype of HGPS cells. Also, Corso and coworkers (128) reported that chromosome 11 alterations are observed at a high frequency in immortalized HGPS cell lines and suggested that these alterations could play a role in escaping senescence.

The amount of progerin in cells is substantially lower than the amount of lamin A and lamin C, yet this small amount of progerin is obviously very potent in terms of causing disease phenotypes in humans and in causing misshapen nuclei in cultured cells. The fact that a small amount of protein causes disastrous consequences has led to the concept that progerin has “dominant negative” (126) or “toxic” (16) effects on cells.

Another point deserves discussion. Although the G608G mutation causing an accumulation of farnesyl-prelamin A is the most common mutation in HGPS patients (15), it is noteworthy that progeroid syndromes with features resembling HGPS can be caused by missense mutations in lamin A/C (15, 99, 129). It is perplexing that different mutations that seemingly yield very different structural al-

Hutchinson-Gilford Progeria Syndrome

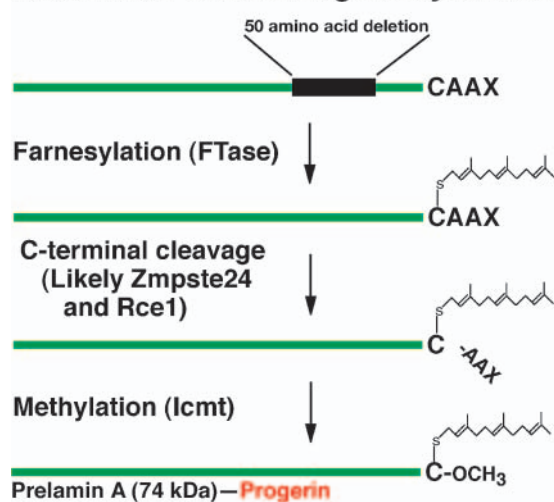


Fig. 21. Production of a mutant prelamin A, progerin, in Hutchinson-Gilford progeria syndrome (HGPS). The 50 amino acid deletion in prelamin A (amino acids 607–656) removes the site for the second endoproteolytic cleavage. Thus, no mature lamin A is formed. Recent data show that progerin is indeed farnesylated (127). We strongly suspect that the AAX of progerin can be cleaved by either Rce1 or Zmpste24 and that the farnesylcysteine is methylated by Icmt.

terations in lamin A/C can cause similar progeria-like phenotypes. One possible interpretation is that the retention of the farnesylcysteine methyl ester in prelamin A is not critical to the emergence of progeria-like disease phenotypes. Another interpretation is that farnesyl-progerin and lamin A/C molecules containing certain amino acid substitutions somehow elicit common structural abnormalities in the lamina. Capanni and coworkers (130) suggested that missense mutations causing progeroid syndromes associated with lipodystrophy elicit an accumulation of prelamin A, which in turn interferes with sterol-regulatory element binding protein metabolism within the cell. However, we have shown that at least some fibroblasts from humans with progeroid disorders have no accumulation of prelamin A (116, 129). In any case, we believe that the missense mutations causing HGPS-like clinical syndromes are exceptionally interesting and critical to understanding progeroid syndromes.

ZMPSTE24 MUTATIONS IN HUMANS CAUSE DISEASE

Soon after the description of bone disease in *Zmpste24*^{-/-} mice (79), MAD was identified as a disease that could be caused by missense mutations in *LMNA* (98). That discovery, along with the realization that *Zmpste24*^{-/-} mice have many MAD-like phenotypes (79), prompted several groups to search for *ZMPSTE24* mutations in MAD patients. In 2003, Agarwal and coworkers (59) identified two *ZMPSTE24* mutations in genomic DNA from a MAD patient with progeroid features and lipodystrophy. DNA sequencing revealed a frameshift mutation, 1085–1086insT (Leu362PhefsX379), as well as a W340R missense mutation in a highly conserved residue immediately adjacent to the zinc metallo-proteinase motif. To determine whether the W340R allele was functional, they expressed the mutant *Zmpste24* in *ste24Δrce1Δ* yeast and assessed **a**-factor production with the halo assay approach described by Tam et al. (47) and Leung et al. (54). The W340R *ZMPSTE24* mutant was capable of promoting **a**-factor production, but the size of the halo appeared to be smaller than with wild-type *ZMPSTE24*, leading the authors to suggest that the W340R mutant had reduced enzymatic activity (59). Unfortunately, quantitative assays of **a**-factor production were not reported. In lieu of quantitative data, it would have been desirable to have documented an accumulation of prelamin A in cultured cells or tissues from the MAD patient, because such data would have unequivocally established a link between the W340R mutation and MAD. Sadly, however, the patient succumbed to his illness, and no tissues or cells were available for analysis (59).

Later, a group in France (131) identified *LMNA* and *ZMPSTE24* mutations in patients with restrictive dermopathy (RD), a lethal perinatal progeroid syndrome characterized by tight and rigid skin with erosions, micrognathia, loss of fat and prominent superficial vasculature, sparse hair, multiple joint contractures, and thin dysplastic clavicles (131). They found that this disorder was caused ei-

ther by *LMNA* mutations that resulted in complete or partial loss of exon 11 sequences or by heterozygous *ZMPSTE24* mutations (notably the Phe361fsX379 mutation). Some of the family members heterozygous for the *ZMPSTE24* mutation were entirely normal. Also, some of the RD patients with the *ZMPSTE24* mutation had an accumulation of prelamin A and an absence of lamin A, as judged from Western blots. The latter findings implied that RD might have been attributable to a complete loss of *ZMPSTE24*; however, the authors concluded that RD was caused by heterozygous *ZMPSTE24* mutations in association with a mutation in another as-yet-unidentified gene (a digenic etiology). Their report (131) spurred Moulson et al. (132), who had been collecting RD patients, to test the hypothesis that RD was caused by homozygous *ZMPSTE24* null mutations. They showed that RD is in fact caused by homozygosity for *ZMPSTE24* null mutations, and they went on to show that RD is associated with a striking increase in prelamin A in cells and misshapen nuclei in cells (132), very much like the situation in mouse *Zmpste24*^{-/-} fibroblasts (16, 83, 116). At about the same time, the French group went back and performed additional DNA sequencing, identified *ZMPSTE24* mutations in both alleles of most RD patients, and revised their conclusions about the genetics of RD (133).

The perinatal lethal phenotype of RD in humans is more severe than the phenotype of *Zmpste24*^{-/-} mice. The milder phenotype in mice is not a great surprise and is consistent with previous studies that have suggested that mice are “tougher” than humans when it comes to structural abnormalities in the nuclear envelope. Thus, mice heterozygous for lamin A/C deficiency (110) or *Lmna* missense mutations are asymptomatic (134, 135), whereas humans with comparable mutations exhibit disease phenotypes (95, 135). Also, mice homozygous for *Lmna* deficiency are viable (95), living for up to 6 weeks, whereas humans lacking lamin A/C are not (113).

Shackleton and coworkers (136) studied another individual with a severe progeroid disease with features of MAD, HGPS, and RD. They excluded *LMNA* mutations and turned to an analysis of *ZMPSTE24*. Sequencing identified the Phe361fsX379 mutation and an N265S missense mutation. Fortunately, skin fibroblasts were available, and Western blots revealed reduced amounts of mature lamin A along with a striking accumulation of prelamin A. By immunofluorescence microscopy, the prelamin A was located at the nuclear periphery and was associated with a high frequency of misshapen nuclei. In this case, it appeared likely that the N265S mutation severely reduced *ZMPSTE24* enzymatic activity.

It seems clear that there is a spectrum of progeroid disorders associated with an accumulation of farnesylated and methylated prelamin A, from the severe neonatal lethal disease RD (with no lamin A biogenesis and an accumulation of farnesyl-prelamin A) (132, 133), to the less severe HGPS (with the accumulation of smaller amounts of a mutant prelamin A from a single mutant *LMNA* allele) (15), to the relatively severe MAD/HGPS case described by Shackleton et al. (136) (with some biogenesis of ma-

ture lamin A but a striking accumulation of prelamin A). We are sometimes asked which is more toxic or more potent in eliciting disease phenotypes, farnesyl-prelamin A in the setting of *ZMPSTE24* deficiency or farnesylated progerin in HGPS. No answers are available in animal studies, but we have compared the percentages of misshapen nuclei in HeLa cells transfected with progerin or a “non-cleavable” full-length prelamin A. In those experiments, progerin appeared to be more potent at eliciting misshapen nuclei (137).

The severity of the progeroid disease phenotypes varies even in patients with the same mutation. In trying to understand this variability, we suggest that it would be a mistake to ignore the experiments by Fong et al. (16), who showed that a single *Lmna* knockout allele can eliminate disease phenotypes caused by *Zmpste24* deficiency. Sooner or later, we suspect that human geneticists will be able to explain at least some of the variability in disease phenotypes in progeroid disorders by genetic factors that control the level of prelamin A accumulation in cells.

TESTING THE CONCEPT THAT FARNESYLATION OF PRELAMIN A COULD BE CRITICAL FOR DISEASE PATHOGENESIS

Shortly after the identification of the HGPS mutation (15), in July 2003, the Progeria Research Foundation, in collaboration with the National Heart, Lung, and Blood Institute and the National Human Genome Research Institute, held a conference to discuss HGPS pathogenesis. The molecular genetics of HGPS were presented, and the possibility that inhibitors of farnesylation might be therapeutically useful was openly discussed. FTIs were initially developed to interfere with the intracellular targeting of mutationally activated Ras proteins (71–74), which are etiologically related to the development of cancer. The Ras proteins are located at the plasma membrane, where they act to stimulate cell division in an uncontrolled manner, ultimately leading to cancer (138, 139). The rationale behind the development of FTIs was to eliminate the farnesyl-lipid anchor from the Ras proteins and thereby mislocalize them away from the plasma membrane and their signaling partners. In the case of HGPS, the idea behind the use of FTIs was similar: to mislocalize progerin away from the nuclear envelope, with the hope that the mislocalization would lessen the ability of the molecule to cause disease. From the beginning, however, nearly everyone recognized that there were potential drawbacks to the FTI approach. For example, these drugs would be expected to interfere with the farnesylation of lamin B1 and lamin B2, conceivably causing further damage to the nuclear lamina (117). In addition, these molecules would be expected to interfere with the farnesylation of dozens of other cellular proteins, conceivably heaping a second insult on already compromised cells. Finally, there was concern that prelamin A might be geranylgeranylated in the setting of an FTI, foiling the overall strategy. [K-Ras is known to be alter-

nately prenylated in the setting of an FTI (140).] Despite these worries, investigators emerged from the conference cautiously optimistic about the possibility of testing FTIs in HGPS.

With funding from the Progeria Research Foundation, work began in several laboratories (<http://www.progeriaresearch.org/grants.shtml>), and by mid-2004, encouraging experimental data were starting to emerge. Also, in late 2004, Fong and coworkers (16) explicitly proposed that the level of farnesyl-prelamin A at the nuclear envelope could be the key to cell toxicity and disease pathogenesis, and they further suggested that reducing the level of the farnesylated form by as little as 50% might be therapeutically useful. This concept clearly resonated and has been restated by others (121, 133).

During the summer of 2005, several groups published results on the effects of FTIs on fibroblasts from patients with HGPS. The first was by Yang and coworkers (117), who tested the ability of a potent FTI to interfere with nuclear shape abnormalities in mouse fibroblasts with a gene-targeted HGPS mutation. They explicitly hypothesized that the salutary effects from blocking the farnesylation of progerin would likely “trump” any potentially deleterious effects on lamin B1 and lamin B2 and lead to an improvement in nuclear shape. Nuclear shape abnormalities in human HGPS fibroblasts had been reported to vary, based in part on passage number. To test the impact of blocking protein farnesylation on the nuclear lamina, Yang et al. (117) reasoned that it might be helpful to create gene-targeted HGPS mice, simply because such a model would make it possible to study the effect of an FTI on nuclear shape in multiple independent lines of low-passage, genetically identical fibroblasts. They created mice carrying a “progerin-only” *Lmna* allele (*Lmna*^{HG/+}) and then immediately proceeded to test the impact of FTI treatment on nuclear shape in cultured fibroblasts. As expected, the percentage of misshapen nuclei in *Lmna*^{HG/+} fibroblasts was increased significantly, compared with that in wild-type fibroblasts (Fig. 22). The results of FTI treatment of *Lmna*^{HG/+} fibroblasts were unequivocal. The FTI mislocalized progerin away from the nuclear envelope to the nucleoplasm, as judged by immunofluorescence microscopy of *Lmna*^{HG/HG} cells (Fig. 23), and quite remarkably, the FTI resulted in a striking improvement in the number of fibroblasts with misshapen nuclei ($P < 0.0001$) (117) (Fig. 24). Remarkably, the drugs did not affect nuclear shape in wild-type fibroblasts (Fig. 24).

Yang and coworkers (117) discussed at some length the interpretation of these results, and in particular whether an FTI might be a reasonable treatment strategy for disease phenotypes in HGPS. Did the favorable effect of FTIs on nuclear shape in *Lmna*^{HG/+} fibroblasts imply that the drugs would likely work to prevent disease phenotypes in humans? In contemplating this question, they suggested that there was room for both optimism and pessimism (117). Optimists would contend that Ockham’s razor dictates that improvements in “whole animal” disease phenotypes would parallel improvements in cellular phenotypes, particularly because nuclear blebbing and whole animal

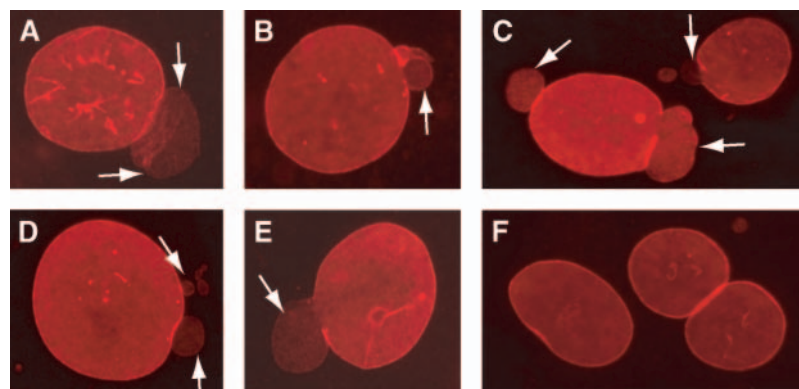


Fig. 22. Frequent misshapen nuclei in *Lmna*^{HG/+} fibroblasts (A–E), and the paucity of misshapen nuclei in wild-type fibroblasts (F). Reproduced, with permission, from *The Proceedings of the National Academy of Sciences USA* (117).

disease phenotypes were clearly associated in studies of *Zmpste24*^{−/−} and *Zmpste24*^{−/−}*Lmna*^{+/−} mice (16). On the other hand, pessimists would argue that lamins are not merely scaffolding proteins but instead interact with a host of nuclear proteins and that it is conceivable that the mechanisms for some HGPS phenotypes might be quite different from the mechanism by which farnesyl-prelamin A perturbs nuclear shape (i.e., that the improvements in nuclear shape abnormalities might just be a completely irrelevant smokescreen). Also, pessimists would argue that FTIs would still leave HGPS cells with an abnormal protein, nonfarnesylated progerin, which still could be toxic in vivo. Along these lines, it is sobering to remember that even single amino acid substitutions in mature lamin A and lamin C, neither of which is farnesylated, can cause a host of different genetic diseases. One could even imagine that an FTI could eliminate progeria but induce another

laminopathy, as a result of the accumulation of nonfarnesylated progerin within cells.

In a follow-up study, Toth et al. (116) tested the ability of FTIs to ameliorate nuclear shape in human fibroblasts from a patient with RD. As in the mouse *Lmna*^{HG/+} fibroblasts, the FTI partially mislocalized prelamin A away from the nuclear envelope (**Fig. 25A, B**). In parallel, the frequency of nuclear shape abnormalities was reduced ($P < 0.0001$) (**Fig. 25C**) (117). Essentially identical results were observed with multiple different mouse *Zmpste24*^{−/−} fibroblasts and in two different human HGPS fibroblast cell lines ($P < 0.0001$) (**Fig. 26**) (117). Capell and colleagues (127) and Glynn and Glover (141) also showed a beneficial effect of an FTI on nuclear shape in human HGPS fibroblasts.

Mallampalli and colleagues (137) made GFP-tagged prelamin A constructs and tested the effects of FTIs in HeLa cells. They tested both a progerin construct and a mutant prelamin A construct with a missense mutation that blocked the endoproteolytic cleavage by ZMPSTE24. Both constructs elicited striking nuclear shape abnormalities in HeLa cells, and these abnormalities were blocked by FTIs (**Fig. 27**) (137). Capell and colleagues (127) performed similar transfection experiments and, importantly, showed that the FTI was ineffective in correcting the nuclear shape abnormalities elicited by a mutant progerin that had been engineered so that it would be geranylgeranlated rather than farnesylated.

The finding that FTIs improve nuclear shape obviously suggests a new paradigm for the treatment of HGPS. It is now essential to further test the effect of FTIs in mouse models of progeria, such as *Zmpste24*^{−/−} mice and the *Lmna*^{HG/+} mice developed by Yang et al. (117). If the results of the mouse experiments are encouraging, the next step would be to test the efficacy of the drugs in human clinical trials.

We suspect that the principal challenge of the mouse experiments, as well as the human clinical trials, will be to administer a sufficiently high dose of an FTI to prevent a large fraction of progerin from being farnesylated. Inhibition of farnesylation with an FTI is often monitored with Western blot assays, either by documenting altered electrophoretic migration of a farnesylated protein, HDJ-2 (142–144), or by documenting the appearance of prelamin A

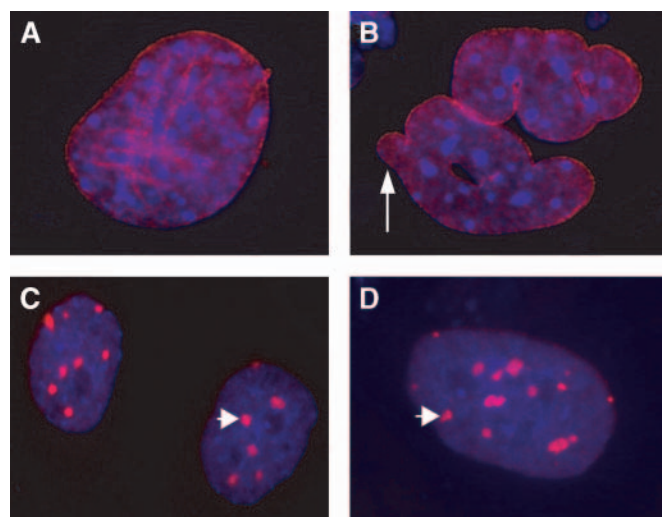


Fig. 23. Immunofluorescence images showing the distribution of progerin in untreated and FTI-treated *Lmna*^{HG/HG} cells. DNA was visualized with 4',6-diamino-phenylindole (blue), and progerin was visualized with an antibody against lamin A (red). A, B: Untreated *Lmna*^{HG/HG} cells, showing progerin along the nuclear envelope. Misshapen nuclei were common (white arrow). C, D: FTI-treated *Lmna*^{HG/HG} cells, revealing intensely staining progerin aggregates (white arrowheads) in the nucleoplasm. Reproduced, with permission, from *The Proceedings of the National Academy of Sciences USA* (117).

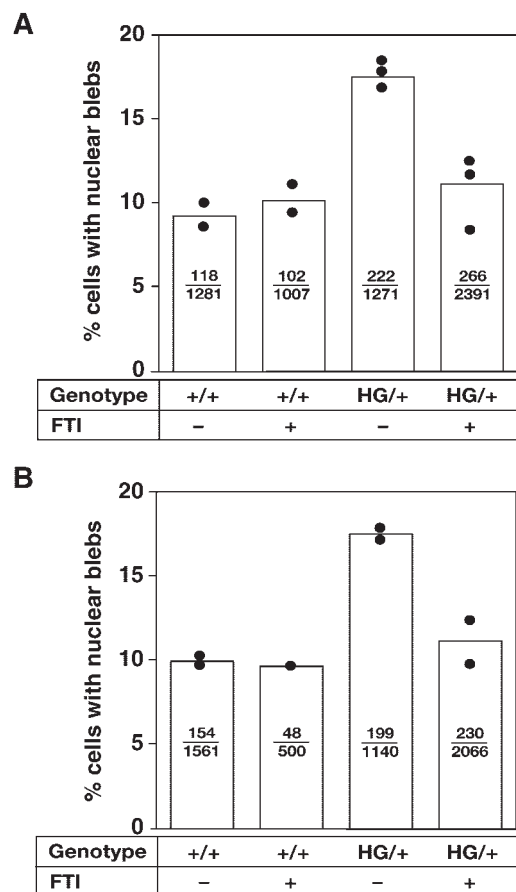


Fig. 24. Bar graphs showing increased frequency of nuclear blebbing in *Lmna*^{HG/+} fibroblasts and a reduction in nuclear blebbing in *Lmna*^{HG/+} fibroblasts treated with an FTI. Results from two independent experiments are shown (A, B). Each black circle shows the frequency of nuclear blebbing with an independently isolated fibroblast cell line. Bars indicate the mean frequency of blebbing; the number of fibroblasts with nuclear blebs and the total number of fibroblasts examined are indicated within each bar. An FTI did not change the frequency of blebbing in *Lmna*^{+/+} fibroblasts. *Lmna*^{HG/+} fibroblasts exhibited more blebbing than *Lmna*^{+/+} fibroblasts ($P < 0.0001$, Chi-square test), and an FTI significantly reduced the frequency of blebbing in *Lmna*^{HG/+} fibroblasts ($P < 0.0001$, Chi-square test). Reproduced, with permission, from *The Proceedings of the National Academy of Sciences USA* (117).

A in cells with the C-terminal prelamins A-specific antibody (144, 145). The problem with the latter Western blot approach, in our experience, is that it is extraordinarily sensitive, and it is quite possible to observe a very strong prelamins A band when there has been very little impact on the overall production of mature lamin A (i.e., when lamin A/C Western blot analysis is performed, there is mainly mature lamin A and only a negligible amount of prelamins A). We suspect that mouse experiments and the human trials will have the best chance of success if the dose of the FTI is adjusted to block 50% of mature lamin A production (as judged by a lamin A/C Western blot), rather than simply using a dose that results in the appearance of prelamins A (with a prelamins A Western blot).

The FTIs are reasonably safe and well-tolerated drugs (142, 146–148) but they have short half-lives, and it is conceivable that the efficacy of FTI therapy in preventing the

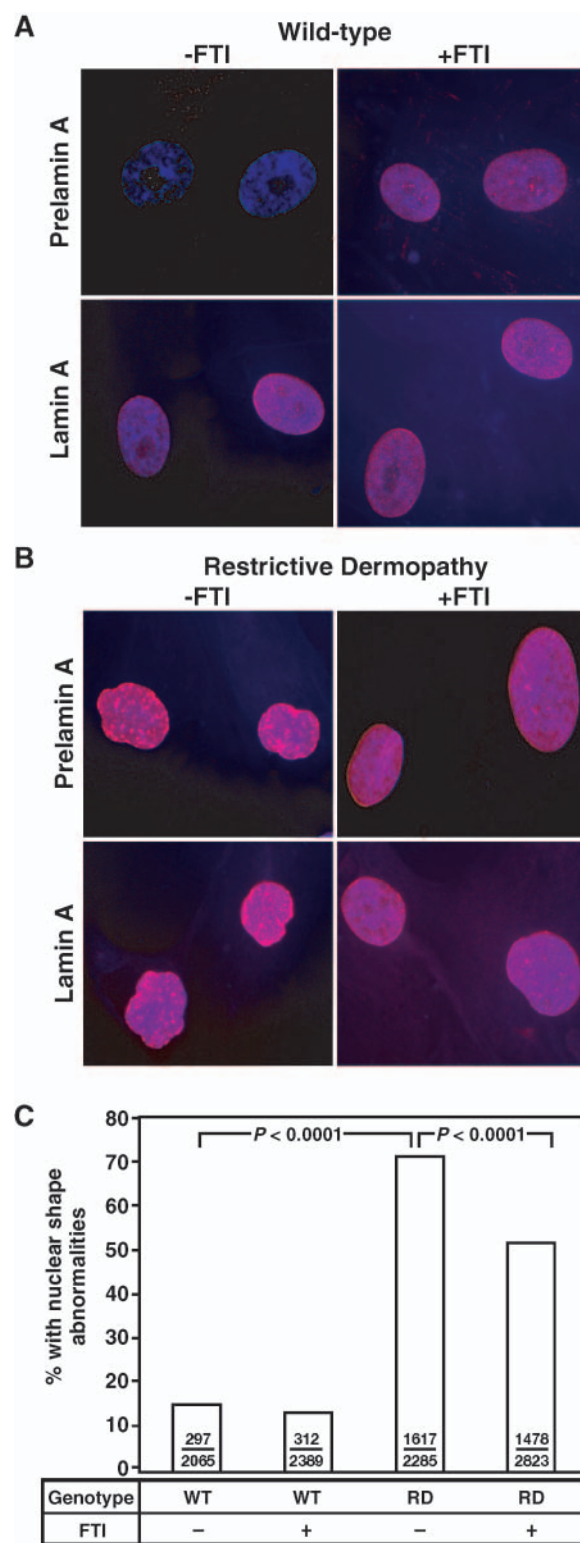


Fig. 25. Effects of an FTI on the localization of prelamins A and on nuclear shape in human wild-type and restrictive dermatopathy (RD) fibroblasts. A, B: Epifluorescence images showing the effects of an FTI on prelamins A and lamin A localization (red) in wild-type (A) and RD (B) fibroblasts. DNA was visualized with 4',6-diaminophenylindole (blue). C: Frequency of misshapen nuclei in wild-type (WT) and RD fibroblasts. Bars show the mean frequency of misshapen nuclei; the number of misshapen nuclei and the total number of nuclei examined are indicated within each bar. An FTI reduced the frequency of misshapen nuclei ($P < 0.0001$, Chi-square test). Reproduced, with permission, from *The Proceedings of the National Academy of Sciences USA* (116).

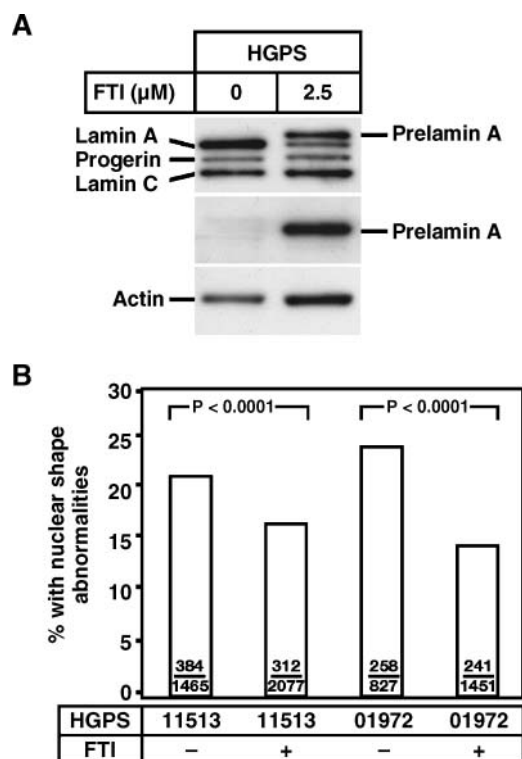


Fig. 26. The effects of an FTI on the frequency of misshapen nuclei in human HGPS fibroblasts. **A:** Western blot analysis of HGPS fibroblasts in the absence or presence of an FTI (PB-43). The antibodies used were anti-lamin A/C polyclonal (top), anti-prelamin A (middle), and anti-actin (bottom). **B:** Impact of an FTI on the frequency of misshapen nuclei in two different HGPS cell lines (AG11513 and AG01972). Reproduced, with permission, from *The Proceedings of the National Academy of Sciences USA* (116).

farnesylation of progerin will require very high trough concentrations of the drug (to block farnesylation “around the clock”). We hope that the side effect profile will make this possible. If not, we believe that there could be a fall-back strategy, one that at least might be helpful for treating the bone abnormalities of HGPS. Nitrogen-containing bisphosphonates, safe drugs commonly used to treat run-of-the-mill osteoporosis, inhibit protein prenylation in bone cells by interfering with farnesyl diphosphate synthase (149, 150), the enzyme that produces farnesyl diphosphate, the cosubstrate for protein farnesyltransferase. These drugs bind avidly to calcium within bone and therefore reach extremely high concentrations in that tissue. They are thought to act by interfering with protein prenylation in bone cells. Toth et al. (116) reasoned that these drugs might be capable of blocking prelamin A farnesylation, thereby interfering with lamin A biogenesis. Indeed, this was the case in both wild-type fibroblasts and HGPS fibroblasts (116). Moreover, these drugs improved the nuclear shape abnormalities in RD fibroblasts (J. Toth, S. G. Young, and L. Fong, unpublished observations). We suspect that these compounds might be very effective in preventing the farnesylation of progerin in the bones of HGPS patients. To the extent that blocking prenylation is important for bone phenotypes, bisphosphonates might be quite useful. Of course, the use of bisphosphonates in

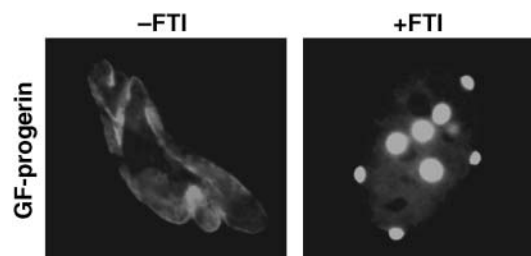


Fig. 27. An FTI (R115777) reverses the nuclear morphology alterations resulting from the expression of GFP-progerin. In the absence of the FTI, most of the HeLa cells contained grossly misshapen nuclei. After FTI treatment, the GFP-progerin invariably localized to foci within the nucleoplasm.

HGPS cannot be recommended without human clinical trials. We suggest that it might be preferable to postpone the testing of bisphosphonates until after the testing of an FTI is completed, inasmuch as the bisphosphonate drugs are retained in bone for months or years and widespread use of these drugs might confound the interpretation of any FTI trials.

MIGHT THERE BE BENEFITS OF FARNESYLTRANSFERASE INHIBITORS FOR OTHER LAMINOPATHIES?

If the FTIs were to ameliorate the disease phenotypes in humans, that would be wonderful for progeria patients and their families. Recently, however, Toth et al. (116) proposed that the utility of FTIs might not be confined to patients with an accumulation of farnesyl-prelamin A in cells. They hypothesized that such drugs might also be useful for patients with other laminopathies caused by missense mutations, in the absence of defective lamin A processing. To test this hypothesis, Toth et al. (116) began by testing whether an FTI might improve the nuclear shape abnormalities in fibroblasts from humans with progeroid syndromes caused by a pair of *LMNA* missense mutations, R644C and E578V (129). The rationale for these audacious experiments was straightforward: that the FTI might improve nuclear shape by preventing the biogenesis of mature lamin A and its appearance at the nuclear envelope (i.e., trading a mutant lamin A at the nuclear envelope for nonfarnesylated prelamin A in the nucleoplasm) (116). Interestingly, they found that nuclear shape was improved. The frequency of misshapen nuclei in R644C fibroblasts was reduced after treatment with an FTI ($P = 0.0003$ and $P = 0.002$ in two experiments); the frequency of misshapen nuclei in E578V fibroblasts was also reduced by the FTI ($P < 0.0001$ in two experiments) (Fig. 28) (116).

The missense mutations that Toth et al. (116) examined, R644C and E578V, are located in the C terminus of lamin A, a region not shared by lamin C. Most disease-causing missense mutations in *LMNA*, however, occur within amino acids 1–566, the region shared by lamin A and lamin C (99, 129). Toth et al. (116) hypothesized that

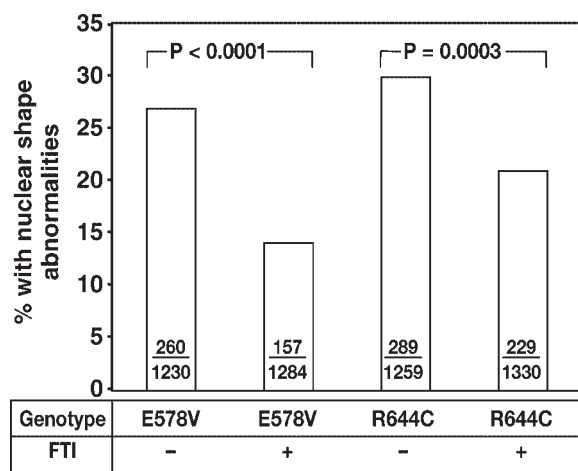


Fig. 28. The impact of an FTI on the frequency of misshapen nuclei in fibroblasts with R644C and E578V mutations. Bars show the mean frequency of misshapen nuclei; the number of misshapen nuclei and the total number of nuclei are indicated within each bar. An FTI reduced the frequency of misshapen nuclei in both mutant cell lines. Reproduced, with permission, from *The Proceedings of the National Academy of Sciences USA* (116).

the FTIs will ultimately be shown to improve nuclear shape in cells with missense mutations shared by lamin A and lamin C, because at the very least the FTIs would be expected to reduce the amount of mature mutant lamin A reaching the nuclear lamina. However, they suggested that the benefit of an FTI might be less impressive with those mutations because the drug might have less impact on the targeting of lamin C. This hypothesis needs to be tested. If the results were favorable, it would be important to test the impact of FTIs on mouse models with *Lmna* mutations and muscular dystrophy and cardiomyopathy (134, 135).

OTHER POTENTIAL STRATEGIES FOR TREATING PROGERIA

There are other potential strategies for treating HGPS, aside from FTIs. In a recent study, Scaffidi and Misteli (151) tested the possibility that a morpholino antisense oligonucleotide specific for progerin might be effective in blocking the aberrant splicing that is at the root of HGPS. They used a morpholino oligonucleotide spanning the mutant splice site (half of the oligonucleotide corresponding to exon 11 sequences and half at the beginning of exon 12). They transfected the oligonucleotide into human HGPS fibroblasts and then used a combination of RT-PCR and Western blot assays to test the possibility that there was a reduction in the mutant HGPS transcript (151). By Western blot, the oligonucleotide clearly caused a reduced amount of mature lamin A in the HGPS cells, and there was a suggestion that the amount of progerin, relative to lamin A, might have been decreased. Notably, two of the phenotypes of HGPS fibroblasts, retarded growth and misshapen nuclei, were ameliorated in cells transfected with the morpholino oligonucleotide. In addition, and quite importantly, the authors identified several genes


with perturbed expression patterns in HGPS fibroblasts and showed, by RNase protection assays, that the expression of those genes was returned toward normal in oligonucleotide-treated fibroblasts (151). The striking improvement in the phenotype of the cells underscored the importance of progerin in causing the hallmark phenotypes in HGPS cells and also suggested a potential therapeutic strategy (151). One question left unresolved by these experiments was the degree to which the salutary effects were attributable to an overall decreased expression of prelamin A, as opposed to a specific effect on mRNA splicing (134, 151).

MOLECULAR MECHANISMS UNDERLYING PROGERIA

The existing evidence suggests that farnesylated progerin in HGPS or farnesylated prelamin A in the case of *Zmpste24* deficiency causes sick cells via a toxic (16) or dominant negative mechanism (126). We believe that the finding of vacuolated osteoblasts (Fig. 17) in *Zmpste24*^{-/-} mice is in agreement with this hypothesis.

The next challenge will be to understand how the accumulation of prelamin A leads to altered gene expression and to the expression of disease phenotypes in certain tissues. Given the importance of the nuclear lamina in the maintenance of the integrity and organization of the nuclear envelope, and the fact that the lamins interact with heterochromatin, transcription factors, and the RNA splicing machinery, this task will be challenging. To begin to approach this issue, Csoka and colleagues (152) performed microarray experiments on HGPS fibroblasts, finding a number of genes with perturbed expression levels, including a number of transcription factors and extracellular matrix proteins. The most affected gene, *MEOX2/GAX*, was a transcription factor that negatively regulates mesodermal tissue proliferation. Scaffidi and Misteli (151) verified some of these gene expression perturbations (for *TIMP3*, *CCL8*, *MMP3*, *HAS3*, and *MMP14*) in HGPS fibroblasts and showed that they were potentially relevant markers of cellular pathology, in that an oligonucleotide designed to interfere with the aberrant mRNA splicing tended to return the expression of these genes toward normal.

Further insights into potential disease mechanisms in progeroid syndromes come from Liu et al. (153). They found that both HGPS and *Zmpste24*^{-/-} fibroblasts exhibited defective DNA repair. This phenotype could be induced by the ectopic expression of a “noncleavable” prelamin A mutant in wild-type fibroblasts. These data suggested that the accumulation of prelamin A might lead directly to defective DNA repair and genome instability, although it remains unclear whether the findings were mechanistically specific to the accumulation of farnesyl-prelamin A. Recently, Varela and colleagues (121) used a genetic approach to study the basis for the accelerated aging phenotypes in *Zmpste24*^{-/-} mice. Microarray experiments revealed that some of the downstream targets of the tumor suppressor gene p53 were upregulated in the setting of

Zmpste24 deficiency, and they hypothesized that activation of p53 signaling events might be one of the mechanisms underlying disease phenotypes in mice. To test this hypothesis, they generated mice deficient in both *Zmpste24* and *p53* (*Zmpste24*^{-/-}*p53*^{-/-}). In these studies, they suggested that the *Zmpste24*^{-/-}*p53*^{-/-} mice exhibited slightly improved longevity and growth rates, compared with *Zmpste24*^{-/-} mice, although the number of mice examined was small and the differences between groups were small. They interpreted their results as showing that overexpression of p53 target genes might be important in disease pathogenesis. Interestingly, similar perturbations in p53 target genes were noted in *Lmna*^{-/-} fibroblasts, in which farnesyl-prelamin A is entirely absent, suggesting that the gene expression differences may have been secondary to major alterations in the nuclear lamina, rather than being specific markers for farnesyl-prelamin A toxicity. In any case, the basic strategy of identifying gene expression perturbations in different tissues, with different genetic abnormalities of the nuclear lamina (e.g., *Lmna*, *Lmnb1*, or *Zmpste24* deficiency), will undoubtedly continue to yield insights into the pathogenesis of progeria as well as other laminopathies. With luck, these insights will be applicable to "normal human aging" and also to a wide spectrum of human diseases. 

The authors thank a talented group of coworkers (Konomi Fujimura-Kamada, Amy Tam, Gordon Leung, Walter Schmidt, Martin Bergo, Meridith Boyle, Monica Mallampalli, Greg Huyer, Julia Toth, Margarita Meta, and Shell Yang) for their dedication to the studies discussed in this article. The authors thank Jan Lammerding, Martin Bergo, Colin Stewart, Steven Clarke, Howard Worman, and Christine Hrycyna for reading the manuscript and making suggestions. The authors thank Brian D. Young for artwork. This work was supported by National Institutes of Health Grants CA-103999, CA-099506, and AR-050200 to S.G.Y. and GM-41223 to S.M. and by grants from the Progeria Research Foundation to S.G.Y., L.G.F., and S.M.

REFERENCES

- Zhang, F. L., and P. J. Casey. 1996. Protein prenylation: molecular mechanisms and functional consequences. *Annu. Rev. Biochem.* **65**: 241–269.
- Clarke, S. 1992. Protein isoprenylation and methylation at carboxyl-terminal cysteine residues. *Annu. Rev. Biochem.* **61**: 355–386.
- Reiss, Y., M. S. Brown, and J. L. Goldstein. 1992. Divalent cation and prenyl pyrophosphate specificities of the protein farnesyltransferase from rat brain, a zinc metalloenzyme. *J. Biol. Chem.* **267**: 6403–6408.
- Seabra, M. C., Y. Reiss, P. J. Casey, M. S. Brown, and J. L. Goldstein. 1991. Protein farnesyltransferase and geranylgeranyltransferase share a common α subunit. *Cell*. **65**: 429–434.
- Pereira-Leal, J. B., and M. C. Seabra. 2000. The mammalian Rab family of small GTPases: definition of family and subfamily sequence motifs suggests a mechanism for functional specificity in the Ras superfamily. *J. Mol. Biol.* **301**: 1077–1087.
- Seabra, M. C., and G. L. James. 1998. Prenylation assays for small GTPases. *Methods Mol. Biol.* **84**: 251–260.
- Seabra, M. C., E. H. Mules, and A. N. Hume. 2002. Rab GTPases, intracellular traffic and disease. *Trends Mol. Med.* **8**: 23–30.
- Brown, M. S., and J. L. Goldstein. 1993. Protein prenylation. Mad bet for Rab. *Nature*. **366**: 14–15.
- Young, S. G., P. Ambroziak, E. Kim, and S. Clarke. 2000. Postisoprenylation protein processing: CXXX (CaaX) endoproteases and isoprenylcysteine carboxyl methyltransferase. In *The Enzymes*. F. Tamanoi and D. S. Sigman, editors. Academic Press, San Diego, CA. 155–213.
- Hrycyna, C. A., and S. Clarke. 1993. Modification of eukaryotic signaling proteins by C-terminal methylation reactions. *Pharmacol. Ther.* **59**: 281–300.
- Lin, F., and H. J. Worman. 1993. Structural organization of the human gene encoding nuclear lamin A and nuclear lamin C. *J. Biol. Chem.* **268**: 16321–16326.
- Mounkes, L. C., B. Burke, and C. L. Stewart. 2001. The A-type lamins. Nuclear structural proteins as a focus for muscular dystrophy and cardiovascular diseases. *Trends Cardiovasc. Med.* **11**: 280–285.
- Burke, B., and C. L. Stewart. 2002. Life at the edge: the nuclear envelope and human disease. *Nat. Rev. Mol. Cell Biol.* **3**: 575–585.
- Hutchison, C. J., and H. J. Worman. 2004. A-type lamins: guardians of the soma? *Nat. Cell Biol.* **6**: 1062–1067.
- Eriksson, M., W. T. Brown, L. B. Gordon, M. W. Glynn, J. Singer, L. Scott, M. R. Erdos, C. M. Robbins, T. Y. Moses, P. Berglund, et al. 2003. Recurrent *de novo* point mutations in lamin A cause Hutchinson-Gilford progeria syndrome. *Nature*. **423**: 293–298.
- Fong, L. G., J. K. Ng, M. Meta, N. Cote, S. H. Yang, C. L. Stewart, T. Sullivan, A. Burghardt, S. Majumdar, K. Reue, et al. 2004. Heterozygosity for *Lmna* deficiency eliminates the progeria-like phenotypes in *Zmpste24*-deficient mice. *Proc. Natl. Acad. Sci. USA*. **101**: 18111–18116.
- Chen, P., S. K. Sapperstein, J. D. Choi, and S. Michaelis. 1997. Biogenesis of the *Saccharomyces cerevisiae* mating pheromone *a*-factor. *J. Cell Biol.* **136**: 251–269.
- Fujimura-Kamada, K., F. J. Nouvet, and S. Michaelis. 1997. A novel membrane-associated metalloprotease, Ste24p, is required for the first step of NH₂-terminal processing of the yeast *a*-factor precursor. *J. Cell Biol.* **136**: 271–285.
- Boyartchuk, V. L., and J. Rine. 1998. Roles of prenyl protein proteases in maturation of *Saccharomyces cerevisiae* *a*-factor. *Genetics*. **150**: 95–101.
- Boyartchuk, V. L., M. N. Ashby, and J. Rine. 1997. Modulation of Ras and *a*-factor function by carboxyl-terminal proteolysis. *Science*. **275**: 1796–1800.
- Hrycyna, C. A., S. K. Sapperstein, S. Clarke, and S. Michaelis. 1991. The *Saccharomyces cerevisiae* STE14 gene encodes a methyltransferase that mediates C-terminal methylation of *a*-factor and Ras proteins. *EMBO J.* **10**: 1699–1709.
- Hrycyna, C. A., and S. Clarke. 1990. Farnesyl cysteine C-terminal methyltransferase activity is dependent upon the STE14 gene product in *Saccharomyces cerevisiae*. *Mol. Cell. Biol.* **10**: 5071–5076.
- Powers, S., S. Michaelis, D. Brock, S. Santa Anna, J. Field, I. Herskowitz, and M. Wigler. 1986. *RAM*, a gene of yeast required for a functional modification of *RAS* proteins and for production of mating pheromone *a*-factor. *Cell*. **47**: 413–422.
- He, B., P. Chen, S.-Y. Chen, K. L. Vancura, S. Michaelis, and S. Powers. 1991. *RAM2*, an essential gene of yeast, and *RAM1* encode the two polypeptide components of the farnesyltransferase that prenylates *a*-factor and Ras proteins. *Proc. Natl. Acad. Sci. USA*. **88**: 11373–11377.
- Casey, P. J. 1992. Biochemistry of protein prenylation. *J. Lipid Res.* **33**: 1731–1740.
- Casey, P. J., and M. C. Seabra. 1996. Protein prenyltransferases. *J. Biol. Chem.* **271**: 5289–5292.
- Schafer, W. R., and J. Rine. 1992. Protein prenylation: genes, enzymes, targets, and functions. *Annu. Rev. Genet.* **30**: 209–237.
- Clarke, S., J. P. Vogel, R. J. Deschenes, and J. Stock. 1988. Post-translational modification of the Ha-ras oncogene protein: evidence for a third class of protein carboxyl methyltransferases. *Proc. Natl. Acad. Sci. USA*. **85**: 4643–4647.
- Dai, Q., E. Choy, V. Chiu, J. Romano, S. R. Slivka, S. A. Steitz, S. Michaelis, and M. R. Philips. 1998. Mammalian prenylcysteine carboxyl methyltransferase is in the endoplasmic reticulum. *J. Biol. Chem.* **273**: 15030–15034.
- Hancock, J. F., A. I. Magee, J. E. Childs, and C. J. Marshall. 1989. All *ras* proteins are polyisoprenylated but only some are palmitoylated. *Cell*. **57**: 1167–1177.
- Caldwell, G. A., F. Naider, and J. M. Becker. 1995. Fungal lipopeptide mating pheromones: a model system for the study of protein prenylation. *Microbiol. Rev.* **59**: 406–422.
- Sapperstein, S., C. Berkower, and S. Michaelis. 1994. Nucleotide

- sequence of the yeast *STE14* gene, which encodes farnesylcysteine carboxyl methyltransferase, and demonstration of its essential role in *a*-factor export. *Mol. Cell. Biol.* **14**: 1438–1449.
33. Bergo, M. O., G. K. Leung, P. Ambroziak, J. C. Otto, P. J. Casey, and S. G. Young. 2000. Targeted inactivation of the isoprenylcysteine carboxyl methyltransferase gene causes mislocalization of K-Ras in mammalian cells. *J. Biol. Chem.* **275**: 17605–17610.
34. Bergo, M. O., B. J. Gavino, C. Hong, A. P. Beigneux, M. McMahon, P. J. Casey, and S. G. Young. 2004. Inactivation of *Icmt* inhibits transformation by oncogenic K-Ras and B-Raf. *J. Clin. Invest.* **113**: 539–550.
35. Kim, E., P. Ambroziak, J. C. Otto, B. Taylor, M. Ashby, K. Shannon, P. J. Casey, and S. G. Young. 1999. Disruption of the mouse *Rce1* gene results in defective Ras processing and mislocalization of Ras within cells. *J. Biol. Chem.* **274**: 8383–8390.
36. Michaelson, D., W. Ali, V. K. Chiu, M. Bergo, J. Silletti, L. Wright, S. G. Young, and M. Philips. 2005. Postprenylation CAAX processing is required for proper localization of Ras but not Rho GTPases. *Mol. Biol. Cell.* **16**: 1606–1616.
37. Sakagami, Y., M. Yoshida, A. Isogai, and A. Suzuki. 1981. Peptidyl sex hormones inducing conjugation tube formation in compatible mating-type cells of *Tremella mesenterica*. *Science*. **212**: 1525–1527.
38. Sakagami, Y., A. Isogai, A. Suzuki, S. Tamura, C. Kitada, and M. Fujino. 1979. Structure of tremorgen A-10, a peptidyl hormone inducing conjugation tube formation in *Tremella mesenterica*. *Agric. Biol. Chem.* **43**: 2643–2645.
39. Kamiya, A., A. Sakurai, S. Tamura, N. Takahashi, E. Tsuchiya, K. Abe, and S. Fukui. 1979. Structure of rhodotorucine A, a peptidyl factor, inducing mating tube formation in *Rhodospiridium toruloides*. *Agric. Biol. Chem.* **43**: 363–369.
40. Ishibashi, Y., Y. Sakagami, A. Isogai, and A. Suzuki. 1984. Structures of tremorgens A-9291-I and A-9291-VIII: peptidyl sex hormones of *Tremella brasiliensis*. *Biochemistry*. **23**: 1399–1404.
41. Ishibashi, Y., Y. Sakagami, A. Isogai, A. Suzuki, and R. J. Bandoni. 1983. Isolation of tremorgens A-9291-I and A-9291-II, novel sex hormones of *Tremella brasiliensis*. *Can. J. Biochem. Cell Biol.* **61**: 796–801.
42. Sprague, G. F., and J. W. Thorner. 1992. Pheromone response and signal transduction during the mating process of *Saccharomyces cerevisiae*. In *The Molecular and Cellular Biology of the Yeast Saccharomyces*. E. W. Jones, J. R. Pringle, and J. R. Broach, editors. Cold Spring Harbor Laboratory Press, Cold Spring Harbor, NY. 657–744.
43. Anderregg, R. J., R. Betz, S. A. Carr, J. W. Crabb, and W. Duntze. 1988. Structure of *Saccharomyces cerevisiae* mating hormone *a*-factor. Identification of S-farnesyl cysteine as a structural component. *J. Biol. Chem.* **263**: 18236–18240.
44. Michaelis, S., and S. Powers. 1988. Biogenesis of yeast mating pheromone *a*-factor and RAS proteins. In *Molecular Biology of Intracellular Protein Sorting and Organelle Assembly*. Alan R. Liss, New York. 193–202.
45. Michaelis, S. 1993. STE6, the yeast *a*-factor transporter. *Semin. Cell Biol.* **4**: 17–27.
46. Schmidt, W. K., A. Tam, K. Fujimura-Kamada, and S. Michaelis. 1998. Endoplasmic reticulum membrane localization of Rce1p and Ste24p, yeast proteases involved in carboxyl-terminal CAAX protein processing and amino-terminal *a*-factor cleavage. *Proc. Natl. Acad. Sci. USA*. **95**: 11175–11180.
47. Tam, A., F. J. Nouvet, K. Fujimura-Kamada, H. Slunt, S. S. Sisodia, and S. Michaelis. 1998. Dual roles for Ste24p in yeast *a*-factor maturation: NH₂-terminal proteolysis and COOH-terminal CAAX processing. *J. Cell Biol.* **142**: 635–649.
48. Schmidt, W. K., A. Tam, and S. Michaelis. 2000. Reconstitution of the Ste24p-dependent N-terminal proteolytic step in yeast *a*-factor biogenesis. *J. Biol. Chem.* **275**: 6227–6233.
49. Tam, A., W. K. Schmidt, and S. Michaelis. 2001. The multispanning membrane protein Ste24p catalyzes CAAX proteolysis and NH₂-terminal processing of the yeast *a*-factor precursor. *J. Biol. Chem.* **276**: 46798–46806.
50. Fujiyama, A., S. Tsunasawa, F. Tamanoi, and F. Sakiyama. 1991. S-farnesylation and methyl esterification of C-terminal domain of yeast RAS2 protein prior to fatty acid acylation. *J. Biol. Chem.* **266**: 17926–17931.
51. Hrycyna, C. A., S. J. Wait, P. S. Backlund, Jr., and S. Michaelis. 1995. Yeast STE14 methyltransferase, expressed as TrpE-STE14 fusion protein in *Escherichia coli*, for *in vitro* carboxylmethylation of prenylated polypeptides. *Methods Enzymol.* **250**: 251–266.
52. Anderson, J. L., H. Frase, S. Michaelis, and C. A. Hrycyna. 2005. Purification, functional reconstitution, and characterization of the *Saccharomyces cerevisiae* isoprenylcysteine carboxylmethyltransferase Ste14p. *J. Biol. Chem.* **280**: 7336–7345.
53. Schmidt, W. K., and S. Michaelis. 2004. Ste24 Protease. In *Handbook of proteolytic enzymes* (2nd edition). A. Barret, N. Rawlings and J. F. Woessner, editors. Academic Press, London. 460–465.
54. Leung, G. K., W. K. Schmidt, M. O. Bergo, B. Gavino, D. H. Wong, A. Tam, M. N. Ashby, S. Michaelis, and S. G. Young. 2001. Biochemical studies of *Zmpste24*-deficient mice. *J. Biol. Chem.* **276**: 29051–29058.
55. Trueblood, C. E., V. L. Boyartchuk, E. A. Picologlou, D. Rozema, C. D. Poulter, and J. Rine. 2000. The CaaX proteases, Afc1p and Rce1p, have overlapping but distinct substrate specificities. *Mol. Cell. Biol.* **20**: 4381–4392.
56. Michaelis, S., and I. Herskowitz. 1988. The *a*-factor pheromone of *Saccharomyces cerevisiae* is essential for mating. *Mol. Cell. Biol.* **8**: 1309–1318.
57. Adames, N., K. Blundell, M. N. Ashby, and C. Boone. 1995. Role of yeast insulin-degrading enzyme homologs in pheromone processing and bud site selection. *Science*. **270**: 464–467.
58. Otto, J. C., E. Kim, S. G. Young, and P. J. Casey. 1999. Cloning and characterization of a mammalian prenyl protein-specific protease. *J. Biol. Chem.* **274**: 8379–8382.
59. Agarwal, A. K., J.-P. Fryns, R. J. Auchus, and A. Garg. 2003. Zinc metalloproteinase, *ZMPSTE24*, is mutated in mandibuloacral dysplasia. *Hum. Mol. Genet.* **12**: 1995–2001.
60. Kumagai, H., Y. Kawamura, K. Yanagisawa, and H. Komano. 1999. Identification of a human cDNA encoding a novel protein structurally related to the yeast membrane-associated metalloprotease, Ste24p. *Biochim. Biophys. Acta*. **1426**: 468–474.
61. Freije, J. M. P., P. Blay, A. M. Pendás, J. Cadiñanos, P. Crespo, and C. López-Otín. 1999. Identification and chromosomal location of two human genes encoding enzymes potentially involved in proteolytic maturation of farnesylated proteins. *Genomics*. **58**: 270–280.
62. Bergo, M. O., G. K. Leung, P. Ambroziak, J. C. Otto, P. J. Casey, A. Q. Gomes, M. C. Seabra, and S. G. Young. 2001. Isoprenylcysteine carboxyl methyltransferase deficiency in mice. *J. Biol. Chem.* **276**: 5841–5845.
63. Maske, C. P., M. S. Hollinshead, N. C. Higbee, M. O. Bergo, S. G. Young, and D. J. Vaux. 2003. A carboxyl-terminal interaction of lamin B1 is dependent on the CAAX endoprotease Rce1 and carboxymethylation. *J. Cell Biol.* **162**: 1223–1232.
64. Bergo, M. O., P. Ambroziak, C. Gregory, A. George, J. C. Otto, E. Kim, H. Nagase, P. J. Casey, A. Balmain, and S. G. Young. 2002. Absence of the CAAX endoprotease Rce1: effects on cell growth and transformation. *Mol. Cell. Biol.* **22**: 171–181.
65. Lin, X., J. Jung, D. Kang, B. Xu, K. S. Zaret, and H. Zoghbi. 2002. Prenylcysteine carboxylmethyltransferase is essential for the earliest stages of liver development in mice. *Gastroenterology*. **123**: 345–351.
66. Smeland, T. E., M. C. Seabra, J. L. Goldstein, and M. S. Brown. 1994. Geranylgeranylated Rab proteins terminating in Cys-Ala-Cys, but not Cys-Cys, are carboxyl-methylated by bovine brain membranes *in vitro*. *Proc. Natl. Acad. Sci. USA*. **91**: 10712–10716.
67. Silvius, J. R., and F. l'Heureux. 1994. Fluorimetric evaluation of the affinities of isoprenylated peptides for lipid bilayers. *Biochemistry*. **33**: 3014–3022.
68. Anderson, J. L., B. S. Henriksen, R. A. Gibbs, and C. A. Hrycyna. 2005. The isoprenoid substrate specificity of isoprenylcysteine carboxylmethyltransferase: development of novel inhibitors. *J. Biol. Chem.* **280**: 29454–29461.
69. Winter-Vann, A. M., and P. J. Casey. 2005. Post-prenylation-processing enzymes as new targets in oncogenesis. *Nat. Rev. Cancer*. **5**: 405–412.
70. Winter-Vann, A. M., R. A. Baron, W. Wong, J. dela Cruz, J. D. York, D. M. Gooden, M. O. Bergo, S. G. Young, E. J. Toone, and P. J. Casey. 2005. A small-molecule inhibitor of isoprenylcysteine carboxyl methyltransferase with antitumor activity in cancer cells. *Proc. Natl. Acad. Sci. USA*. **102**: 4336–4341.
71. Kohl, N. E., F. R. Wilson, S. D. Mosser, E. Giuliani, S. J. DeSolms, M. W. Conner, N. J. Anthony, W. J. Holtz, R. P. Gomez, T. J. Lee, et al. 1994. Protein farnesyltransferase inhibitors block the growth of *ras*-dependent tumors in nude mice. *Proc. Natl. Acad. Sci. USA*. **91**: 9141–9145.
72. Gibbs, J. B., A. Oliff, and N. E. Kohl. 1994. Farnesyltransferase inhibitors: Ras research yields a potential cancer therapeutic. *Cell*. **77**: 175–178.
73. Tamanoi, F. 1993. Inhibitors of Ras farnesyltransferases. *Trends Biochem. Sci.* **18**: 349–353.
74. James, G. L., J. L. Goldstein, M. S. Brown, T. E. Rawson, T. C. Som-

- ers, R. S. McDowell, C. W. Crowley, B. K. Lucas, A. D. Levinson, and J. C. Marsters, Jr. 1993. Benzodiazepine peptidomimetics: potent inhibitors of Ras farnesylation in animal cells. *Science*. **260**: 1937–1942.
75. Schmidt, R. A., C. J. Schneider, and J. A. Glomset. 1984. Evidence for post-translational incorporation of a product of mevalonic acid into Swiss 3T3 cell proteins. *J. Biol. Chem.* **259**: 10175–10180.
76. Glomset, J. A., and C. C. Farnsworth. 1994. Role of protein modification reactions in programming interactions between ras-related GTPases and cell membranes. *Annu. Rev. Cell Biol.* **10**: 181–205.
77. Kim, C. M., J. L. Goldstein, and M. S. Brown. 1992. cDNA cloning of MEV, a mutant protein that facilitates cellular uptake of mevalonate, and identification of the point mutation responsible for its gain of function. *J. Biol. Chem.* **267**: 23113–23121.
78. Wilson, K. L. 2000. The nuclear envelope, muscular dystrophy and gene expression. *Trends Cell Biol.* **10**: 125–129.
79. Bergo, M. O., B. Gavino, J. Ross, W. K. Schmidt, C. Hong, L. V. Kendall, A. Mohr, M. Meta, H. Genant, Y. Jiang, et al. 2002. *Zmpste24* deficiency in mice causes spontaneous bone fractures, muscle weakness, and a prelamin A processing defect. *Proc. Natl. Acad. Sci. USA*. **99**: 13049–13054.
80. Bergo, M. O., and S. G. Young. 2005. *Zmpste24* (mammalian farnesylated protein-converting enzyme 1). In *Handbook of Proteolytic Enzymes*. A. J. Barrett, N. D. Rawlings, and J. F. Woessner, editors. Academic Press, London. In press.
81. Corrigan, D. P., D. Kuszcak, A. E. Rusinol, D. P. Thewke, C. A. Hrycyna, S. Michaelis, and M. S. Sinensky. 2005. Prelamin A endoproteolytic processing in vitro by recombinant *Zmpste24*. *Biochem. J.* **387**: 129–138.
82. Kilic, F., M. B. Dalton, S. K. Burrell, J. P. Mayer, S. D. Patterson, and M. Sinensky. 1997. *In vitro* assay and characterization of the farnesylation-dependent prelamin A endoprotease. *J. Biol. Chem.* **272**: 5298–5304.
83. Pendás, A. M., Z. Zhou, J. Cadiñanos, J. M. P. Freije, J. Wang, K. Hultenby, A. Astudillo, A. Wernerson, F. Rodríguez, K. Tryggvason, et al. 2002. Defective prelamin A processing and muscular and adipocyte alterations in *Zmpste24* metalloproteinase-deficient mice. *Nat. Genet.* **31**: 94–99.
84. Fisher, D. Z., N. Chaudhary, and G. Blobel. 1986. cDNA sequencing of nuclear lamins A and C reveals primary and secondary structural homology to intermediate filament proteins. *Proc. Natl. Acad. Sci. USA*. **83**: 6450–6454.
85. Chelsky, D., C. Sobotka, and C. L. O'Neill. 1989. Lamin B methylation and assembly into the nuclear envelope. *J. Biol. Chem.* **264**: 7637–7643.
86. Izumi, M., O. A. Vaughan, C. J. Hutchison, and D. M. Gilbert. 2000. Head and/or CaaX domain deletions of lamin proteins disrupt preformed lamin A and C but not lamin B structure in mammalian cells. *Mol. Biol. Cell*. **11**: 4323–4337.
87. Beck, L. A., T. J. Hosick, and M. Sinensky. 1990. Isoprenylation is required for the processing of the lamin A precursor. *J. Cell Biol.* **110**: 1489–1499.
88. Hennekes, H., and E. A. Nigg. 1994. The role of isoprenylation in membrane attachment of nuclear lamins. A single point mutation prevents proteolytic cleavage of the lamin A precursor and confers membrane binding properties. *J. Cell Sci.* **107**: 1019–1029.
89. Vaughan, O. A., M. Alvarez-Reyes, J. M. Bridger, J. L. V. Broers, F. C. S. Ramaekers, M. Wehnert, G. E. Morris, W. G. F. Whitfield, and C. J. Hutchison. 2001. Both emerin and lamin C depend on lamin A for localization at the nuclear envelope. *J. Cell Sci.* **114**: 2577–2590.
90. Dalton, M., and M. Sinensky. 1995. Expression systems for nuclear lamin proteins: farnesylation in assembly of nuclear lamina. *Methods Enzymol.* **250**: 134–148.
91. Kilic, F., D. A. Johnson, and M. Sinensky. 1999. Subcellular localization and partial purification of prelamin A endoprotease: an enzyme which catalyzes the conversion of farnesylated prelamin A to mature lamin A. *FEBS Lett.* **450**: 61–65.
92. Hegele, R. A. 2000. Familial partial lipodystrophy: a monogenic form of the insulin resistance syndrome. *Mol. Genet. Metab.* **71**: 539–544.
93. Hegele, R. A. 2001. Molecular basis of partial lipodystrophy and prospects for therapy. *Trends Mol. Med.* **7**: 121–126.
94. Garg, A. 2000. Lipodystrophies. *Am. J. Med.* **108**: 143–152.
95. Bonne, G., M. R. Di Barletta, S. Varnous, H-M. Bécan, E-H. Hammouda, L. Merlini, F. Muntioni, C. R. Greenberg, F. Gary, J-A. Urtizberea, et al. 1999. Mutations in the gene encoding lamin A/C cause autosomal dominant Emery-Dreifuss muscular dystrophy. *Nat. Genet.* **21**: 285–288.
96. Vytöpil, M., S. Benedetti, E. Ricci, G. Galluzzi, A. D. Russo, L. Merlini, G. Boriani, M. Gallina, L. Morandi, L. Politano, et al. 2003. Mutation analysis of the lamin A/C gene (LMNA) among patients with different cardiomyopathic phenotypes. *J. Med. Genet.* **40**: 132.
97. De Sandre-Giovannoli, A., M. Chaouch, S. Kozlov, J-M. Vallat, M. Tazir, N. Kassouri, P. Szepietowski, T. Hammadouche, A. Vandenberghe, C. L. Stewart, et al. 2002. Homozygous defects in LMNA, encoding lamin A/C nuclear-envelope proteins, cause autosomal recessive axonal neuropathy in human (Charcot-Marie-Tooth disorder type 2) and mouse. *Am. J. Hum. Genet.* **70**: 726–736.
98. Novelli, G., A. Muchir, F. Sangiulio, A. Helbling-Leclerc, M. R. D'Apice, C. Massart, F. Capon, P. Sbraccia, M. Federici, R. Lauro, et al. 2002. Mandibuloacral dysplasia is caused by a mutation in LMNA-encoding lamin A/C. *Am. J. Hum. Genet.* **71**: 426–431.
99. Chen, L., L. Lee, B. A. Kudlow, H. G. Dos Santos, O. Sletvold, Y. Shafeghati, E. G. Botha, A. Garg, N. B. Hanson, G. M. Martin, et al. 2003. LMNA mutations in atypical Werner's syndrome. *Lancet*. **362**: 440–445.
100. Hegele, R. A. 2003. Drawing the line in progeria syndromes. *Lancet*. **362**: 416–417.
101. Dhe-Paganon, S., E. D. Werner, Y-I. Chi, and S. E. Shoelson. 2002. Structure of the globular tail of nuclear lamin. *J. Biol. Chem.* **277**: 17381–17384.
102. Krimm, I., C. Ostlund, B. Gilquin, J. Couprie, P. Hossenlopp, J. P. Mornon, G. Bonne, J. C. Courvalin, H. J. Worman, and S. Zinn-Justin. 2002. The Ig-like structure of the C-terminal domain of lamin A/C, mutated in muscular dystrophies, cardiomyopathy, and partial lipodystrophy. *Structure (Camb)*. **10**: 811–823.
103. Garg, A., O. Cogulu, F. Ozkinay, H. Onay, and A. K. Agarwal. 2005. A novel homozygous Ala529Val LMNA mutation in Turkish patients with mandibuloacral dysplasia. *J. Clin. Endocrinol. Metab.* **90**: 5259–5264.
104. Muchir, A., J. Medioni, M. Laluc, C. Massart, T. Arimura, A. J. van der Kooi, I. Desguerre, M. Mayer, X. Ferrer, S. Briault, et al. 2004. Nuclear envelope alterations in fibroblasts from patients with muscular dystrophy, cardiomyopathy, and partial lipodystrophy carrying lamin A/C gene mutations. *Muscle Nerve*. **30**: 444–450.
105. Wilson, K. L., M. S. Zastrow, and K. K. Lee. 2001. Lamins and disease: insights into nuclear infrastructure. *Cell*. **104**: 647–650.
106. Hutchison, C. J., M. Alvarez-Reyes, and O. A. Vaughan. 2001. Lamins in disease: why do ubiquitously expressed nuclear envelope proteins give rise to tissue-specific disease phenotypes? *J. Cell Sci.* **114**: 9–19.
107. Lammerding, J., P. C. Schulze, T. Takahashi, S. Kozlov, T. Sullivan, R. D. Kamm, C. L. Stewart, and R. T. Lee. 2004. Lamin A/C deficiency causes defective nuclear mechanics and mechanotransduction. *J. Clin. Invest.* **113**: 370–378.
108. Broers, J. L., E. A. Peeters, H. J. Kuipers, J. Endert, C. V. Bouten, C. W. Oomens, F. P. Baaijens, and F. C. Ramaekers. 2004. Decreased mechanical stiffness in LMNA^{-/-} cells is caused by defective nucleocytoplasmic integrity: implications for the development of laminopathies. *Hum. Mol. Genet.* **13**: 2567–2580.
109. Vergnes, L., M. Peterfy, M. O. Bergo, S. G. Young, and K. Reue. 2004. Lamin B1 is required for mouse development and nuclear integrity. *Proc. Natl. Acad. Sci. USA*. **101**: 10428–10433.
110. Sullivan, T., D. Escalante-Alcalde, H. Bhatt, M. Anver, N. Bhat, K. Nagashima, C. L. Stewart, and B. Burke. 1999. Loss of A-type lamin expression compromises nuclear envelope integrity leading to muscular dystrophy. *J. Cell Biol.* **147**: 913–919.
111. Cutler, D. A., T. Sullivan, B. Marcus-Samuels, C. L. Stewart, and M. L. Reitman. 2002. Characterization of adiposity and metabolism in *Lmna*-deficient mice. *Biochem. Biophys. Res. Commun.* **291**: 522–527.
112. Raharjo, W. H., P. Enarson, T. Sullivan, C. L. Stewart, and B. Burke. 2001. Nuclear envelope defects associated with LMNA mutations cause dilated cardiomyopathy and Emery-Dreifuss muscular dystrophy. *J. Cell Sci.* **114**: 4447–4457.
113. Muchir, A., B. G. van Engelen, M. Lammens, J. M. Mislow, E. McNally, K. Schwartz, and G. Bonne. 2003. Nuclear envelope alterations in fibroblasts from LGMD1B patients carrying nonsense Y259X heterozygous or homozygous mutation in lamin A/C gene. *Exp. Cell Res.* **291**: 352–362.
114. Weber, K., U. Plessmann, and P. Traub. 1989. Maturation of nuclear lamin A involves a specific carboxy-terminal trimming, which removes the polyisoprenylation site from the precursor: implications for the structure of the nuclear lamina. *FEBS Lett.* **257**: 411–414.
115. Young, S. G., S. Clarke, M. Bergo, M. Philips, and L. G. Fong. 2005. Genetic approaches to understanding the physiologic im-

- portance of the carboxyl methylation of isoprenylated proteins. *The Enzymes*. In press.
116. Toth, J. I., S. H. Yang, X. Qiao, A. P. Beigneux, M. H. Gelb, C. L. Moulson, J. H. Miner, S. G. Young, and L. G. Fong. 2005. Blocking protein farnesyltransferase improves nuclear shape in fibroblasts from humans with progeroid syndromes. *Proc. Natl. Acad. Sci. USA*. **102**: 12873–12878.
 117. Yang, S. H., M. O. Bergo, J. I. Toth, X. Qiao, Y. Hu, S. Sandoval, M. Meta, P. Bendale, M. H. Gelb, S. G. Young, et al. 2005. Blocking protein farnesyltransferase improves nuclear blebbing in mouse fibroblasts containing a targeted Hutchinson-Gilford progeria syndrome mutation. *Proc. Natl. Acad. Sci. USA*. **102**: 10291–10296.
 118. Cahill, G. F., Jr. 1970. Starvation in man. *N. Engl. J. Med.* **282**: 668–675.
 119. Mounkes, L. C., S. Kozlov, L. Hernandez, T. Sullivan, and C. L. Stewart. 2003. A progeroid syndrome in mice is caused by defects in A-type lamins. *Nature*. **423**: 298–301.
 120. Olson, E. N., H-H. Arnold, P. W. J. Rigby, and B. J. Wold. 1996. Know your neighbors: three phenotypes in null mutants of the myogenic bHLH gene *MRF4*. *Cell*. **85**: 1–4.
 121. Varela, I., J. Cadinanos, A. M. Pendas, A. Gutierrez-Fernandez, A. R. Folgueras, L. M. Sanchez, Z. Zhou, F. J. Rodriguez, C. L. Stewart, J. A. Vega, et al. 2005. Accelerated ageing in mice deficient in *Zmpste24* protease is linked to p53 signalling activation. *Nature*. **437**: 564–568.
 122. Debusk, F. L., B. Burke, and C. L. Stewart. 1972. The Hutchinson-Gilford progeria syndrome. *J. Pediatr.* **80**: 697–724.
 123. Cao, H., and R. A. Hegele. 2003. LMNA is mutated in Hutchinson-Gilford progeria (MIM 176670) but not in Wiedemann-Rautenstrauch progeroid syndrome (MIM 264090). *J. Hum. Genet.* **48**: 271–274.
 124. de Sandre-Giovannoli, A., R. Bernard, P. Cau, C. Navarro, J. Amiel, I. Boccaccio, S. Lyonnet, C. L. Stewart, A. Munnich, M. Le Merrer, et al. 2003. Lamin A truncation in Hutchinson-Gilford progeria. *Science*. **300**: 2055.
 125. Reddel, C. J., and A. S. Weiss. 2004. Lamin A expression levels are unperturbed at the normal and mutant alleles but display partial splice site selection in Hutchinson-Gilford progeria syndrome. *J. Med. Genet.* **41**: 715–717.
 126. Goldman, R. D., D. K. Shumaker, M. R. Erdos, M. Eriksson, A. E. Goldman, L. B. Gordon, Y. Gruenbaum, S. Khuon, M. Mendez, R. Varga, et al. 2004. Accumulation of mutant lamin A causes progressive changes in nuclear architecture in Hutchinson-Gilford progeria syndrome. *Proc. Natl. Acad. Sci. USA*. **101**: 8963–8968.
 127. Capell, B. C., M. R. Erdos, J. P. Madigan, J. J. Fiordalisi, R. Varga, K. N. Conneely, L. B. Gordon, C. J. Der, A. D. Cox, and F. S. Collins. 2005. Inhibiting farnesylation of progerin prevents the characteristic nuclear blebbing of Hutchinson-Gilford progeria syndrome. *Proc. Natl. Acad. Sci. USA*. **102**: 12879–12884.
 128. Corso, C., E. M. Parry, R. G. Faragher, A. Seager, M. H. Green, and J. M. Parry. 2005. Molecular cytogenetic insights into the ageing syndrome Hutchinson-Gilford progeria (HGPS). *Cytogenet. Genome Res.* **111**: 27–33.
 129. Csoka, A. B., H. Cao, P. J. Sammak, D. Constantinescu, G. P. Schatten, and R. A. Hegele. 2004. Novel lamin A/C gene (LMNA) mutations in atypical progeroid syndromes. *J. Med. Genet.* **41**: 304–308.
 130. Capanni, C., E. Mattioli, M. Columbaro, E. Lucarelli, V. K. Parnai, G. Novelli, M. Wehnert, V. Cenni, N. M. Maraldi, S. Squarzon, et al. 2005. Altered pre-lamin A processing is a common mechanism leading to lipodystrophy. *Hum. Mol. Genet.* **14**: 1489–1502.
 131. Navarro, C., A. D. Sandre-Giovannoli, R. Bernard, I. Boccaccio, A. Boyer, D. Genevieve, S. Hadj-Rabia, C. Gaudy-Marqueste, H. S. Smitt, P. Vabres, et al. 2004. Lamin A and ZMPSTE24 defects cause nuclear disorganization and identify restrictive dermatopathy as a lethal neonatal laminopathy. *Hum. Mol. Gen.* **13**: 2493–2503.
 132. Moulson, C. L., G. Go, J. M. Gardner, A. C. van der Wal, J. H. S. Smitt, J. M. van Hagen, and J. H. Miner. 2005. Homozygous and compound heterozygous mutations in *ZMPSTE24* cause the laminopathy restrictive dermatopathy. *J. Invest. Dermatol.* In press.
 133. Navarro, C. L., J. Cadinanos, A. De Sandre-Giovannoli, R. Bernard, S. Courrier, I. Boccaccio, A. Boyer, W. J. Kleijer, A. Wagner, F. Giuliano, et al. 2005. Loss of ZMPSTE24 (FACE-1) causes autosomal recessive restrictive dermatopathy and accumulation of lamin A precursors. *Hum. Mol. Genet.* **14**: 1503–1513.
 134. Mounkes, L. C., S. V. Kozlov, J. N. Rottman, and C. L. Stewart. 2005. Expression of an LMNA-N195K variant of A-type lamins results in cardiac conduction defects and death in mice. *Hum. Mol. Genet.* **14**: 2167–2180.
 135. Arimura, T., A. Helbling-Leclerc, C. Massart, S. Varnous, F. Niel, E. Lacene, Y. Fromes, M. Toussaint, A. M. Mura, D. I. Keller, et al. 2005. Mouse model carrying H222P-Lmna mutation develops muscular dystrophy and dilated cardiomyopathy similar to human striated muscle laminopathies. *Hum. Mol. Genet.* **14**: 155–169.
 136. Shackleton, S., D. T. Smallwood, P. Clayton, L. C. Wilson, A. K. Agarwal, A. Garg, and R. C. Trembath. 2005. Compound heterozygous ZMPSTE24 mutations reduce prelamin A processing and result in a severe progeroid phenotype. *J. Med. Genet.* **42**: e36.
 137. Mallampalli, M. P., G. Huyer, P. Bendale, M. H. Gelb, and S. Michaelis. 2005. Inhibiting farnesylation reverses the nuclear morphology defect in a HeLa cell model for Hutchinson-Gilford progeria syndrome. *Proc. Natl. Acad. Sci. USA*. **102**: 14416–14421.
 138. Rodenhuis, S. 1992. *ras* and human tumors. *Semin. Cancer Biol.* **3**: 241–247.
 139. Bos, J. L. 1989. *ras* oncogenes in human cancer: a review. *Cancer Res.* **49**: 4682–4689.
 140. Whyte, D. B., P. Kirschmeier, T. N. Hockenberry, I. Nunez-Oliva, L. James, J. J. Catino, W. R. Bishop, and J.-K. Pai. 1997. K- and N-Ras are geranylgeranylated in cells treated with farnesyl protein transferase inhibitors. *J. Biol. Chem.* **272**: 14459–14464.
 141. Glynn, M. W., and T. W. Glover. 2005. Incomplete processing of mutant lamin A in Hutchinson-Gilford progeria leads to nuclear abnormalities, which are reversed by farnesyltransferase inhibition. *Hum. Mol. Genet.* **14**: 2959–2969.
 142. Alsina, M., R. Fonseca, E. F. Wilson, A. N. Belle, E. Gerbino, T. Price-Troska, R. M. Overton, G. Ahmann, L. M. Bruzek, A. A. Adjei, et al. 2004. Farnesyltransferase inhibitor tipifarnib is well tolerated, induces stabilization of disease, and inhibits farnesylation and oncogenic/tumor survival pathways in patients with advanced multiple myeloma. *Blood*. **103**: 3271–3277.
 143. Izbicka, E., D. Campos, G. Carrizales, and A. Patnaik. 2005. Biomarkers of anticancer activity of R115777 (tipifarnib, zarvestra) in human breast cancer models in vitro. *Anticancer Res.* **25**: 3215–3223.
 144. Adjei, A. A., J. N. Davis, C. Erlichman, P. A. Svingen, and S. H. Kaufmann. 2000. Comparison of potential markers of farnesyltransferase inhibition. *Clin. Cancer Res.* **6**: 2318–2325.
 145. Adjei, A. A., G. A. Croghan, C. Erlichman, R. S. Marks, J. M. Reid, J. A. Sloan, H. C. Pitot, S. R. Alberts, R. M. Goldberg, L. J. Hanson, et al. 2003. A phase I trial of the farnesyl protein transferase inhibitor R115777 in combination with gemcitabine and cisplatin in patients with advanced cancer. *Clin. Cancer Res.* **9**: 2520–2526.
 146. Kim, E. S., M. S. Kies, F. V. Fossella, B. S. Glisson, S. Zaknoen, P. Statkevich, R. F. Munden, C. Summey, K. M. Pisters, V. Papadimitrakopoulou, et al. 2005. Phase II study of the farnesyltransferase inhibitor lonafarnib with paclitaxel in patients with taxane-refractory/resistant nonsmall cell lung carcinoma. *Cancer*. **104**: 561–569.
 147. Ferguson, D., L. E. Rodriguez, J. P. Palma, M. Refici, K. Jarvis, J. O'Connor, G. M. Sullivan, D. Frost, K. Marsh, J. Bauch, et al. 2005. Antitumor activity of orally bioavailable farnesyltransferase inhibitor, ABT-100, is mediated by antiproliferative, proapoptotic, and antiangiogenic effects in xenograft models. *Clin. Cancer Res.* **11**: 3045–3054.
 148. Rao, S., D. Cunningham, A. de Gramont, W. Scheithauer, M. Smakal, Y. Humblet, G. Kourteva, T. Iveson, T. Andre, J. Dostalova, et al. 2004. Phase III double-blind placebo-controlled study of farnesyl transferase inhibitor R115777 in patients with refractory advanced colorectal cancer. *J. Clin. Oncol.* **22**: 3950–3957.
 149. Oades, G. M., S. G. Senaratne, I. A. Clarke, R. S. Kirby, and K. W. Colston. 2003. Nitrogen containing bisphosphonates induce apoptosis and inhibit the mevalonate pathway, impairing Ras membrane localization in prostate cancer cells. *J. Urol.* **170**: 246–252.
 150. Rogers, M. J. 2003. New insights into the molecular mechanisms of action of bisphosphonates. *Curr. Pharm. Des.* **9**: 2643–2658.
 151. Scaffidi, P., and T. Misteli. 2005. Reversal of the cellular phenotype in the premature aging disease Hutchinson-Gilford progeria syndrome. *Nat. Med.* **11**: 440–445.
 152. Csoka, A. B., S. B. English, C. P. Simkevich, D. G. Ginzinger, A. J. Butte, G. P. Schatten, F. G. Rothman, and J. M. Sedivy. 2004. Genome-scale expression profiling of Hutchinson-Gilford progeria syndrome reveals widespread transcriptional misregulation leading to mesodermal/mesenchymal defects and accelerated atherosclerosis. *Aging Cell*. **3**: 235–243.
 153. Liu, B., J. Wang, K. M. Chan, W. M. Tjia, W. Deng, X. Guan, J. D. Huang, K. M. Li, P. Y. Chau, D. J. Chen, et al. 2005. Genomic instability in laminopathy-based premature aging. *Nat. Med.* **11**: 780–785.